

## Coordination to Imidazole Ring Switches On Phosphorescence of Platinum Cyclometalated Complexes: The Route to Selective Labeling of Peptides and Proteins via Histidine Residues

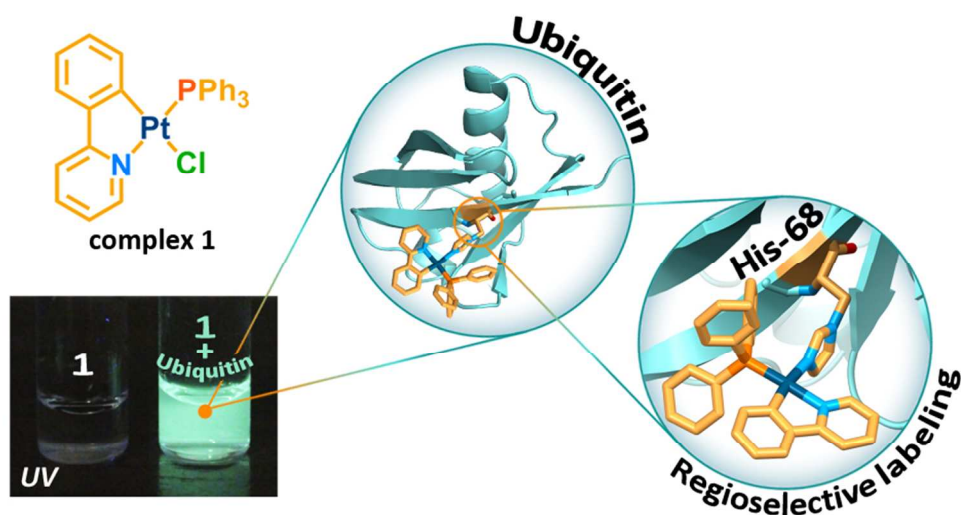
Anastasia I. Solomatina, Pavel S Chelushkin, Dmitrii V. Krupenya, Ivan S. Podkorytov, Tatiana O. Artamonova, Vladimir V. Sizov, Alexei S Melnikov, Vladislav V. Gurzhiy, Elena I. Koshel, Vladislav Shcheslavskiy, and Sergey P Tunik

*Bioconjugate Chem.*, **Just Accepted Manuscript** • DOI: 10.1021/acs.bioconjchem.6b00598 • Publication Date (Web): 15 Nov 2016

Downloaded from <http://pubs.acs.org> on November 19, 2016

### Just Accepted

“Just Accepted” manuscripts have been peer-reviewed and accepted for publication. They are posted online prior to technical editing, formatting for publication and author proofing. The American Chemical Society provides “Just Accepted” as a free service to the research community to expedite the dissemination of scientific material as soon as possible after acceptance. “Just Accepted” manuscripts appear in full in PDF format accompanied by an HTML abstract. “Just Accepted” manuscripts have been fully peer reviewed, but should not be considered the official version of record. They are accessible to all readers and citable by the Digital Object Identifier (DOI®). “Just Accepted” is an optional service offered to authors. Therefore, the “Just Accepted” Web site may not include all articles that will be published in the journal. After a manuscript is technically edited and formatted, it will be removed from the “Just Accepted” Web site and published as an ASAP article. Note that technical editing may introduce minor changes to the manuscript text and/or graphics which could affect content, and all legal disclaimers and ethical guidelines that apply to the journal pertain. ACS cannot be held responsible for errors or consequences arising from the use of information contained in these “Just Accepted” manuscripts.



25 Table of Content graphics

26 82x44mm (300 x 300 DPI)

27  
28  
29  
30  
31  
32  
33  
34  
35  
36  
37  
38  
39  
40  
41  
42  
43  
44  
45  
46  
47  
48  
49  
50  
51  
52  
53  
54  
55  
56  
57  
58  
59  
60

# Coordination to Imidazole Ring Switches On Phosphorescence of Platinum Cyclometalated Complexes: The Route to Selective Labeling of Peptides and Proteins *via* Histidine Residues

Anastasia I. Solomatina,<sup>†</sup> Pavel S. Chelushkin,<sup>†,‡</sup> Dmitrii V. Krupenya,<sup>†</sup> Ivan S. Podkorytov,<sup>‡</sup> Tatiana O. Artamonova,<sup>#</sup> Vladimir V. Sizov,<sup>†</sup> Alexei S. Melnikov,<sup>§,#</sup> Vladislav V. Gurzhiy,<sup>°</sup> Elena I. Koshel,<sup>‡</sup> Vladislav I. Shcheslavskiy,<sup>´</sup> Sergey P. Tunik<sup>\*,†</sup>

<sup>†</sup>St. Petersburg State University, Institute of Chemistry, Universitetskii pr. 26, 198504, St. Petersburg, Russia

<sup>‡</sup>Institute of Macromolecular Compounds, Russian Academy of Sciences, Bolshoi pr. V.O., 31, 199004, St. Petersburg, Russia

<sup>§</sup>St. Petersburg State University, Department of Physics, Ulianovskaya Str., 3, 198504, St. Petersburg, Russia

<sup>‡</sup>St. Petersburg State University, Biomolecular NMR Laboratory, Botanicheskaya 17, St. Petersburg 198504, Russia

<sup>#</sup>Peter the Great St. Petersburg Polytechnic University, Research center of nanobiotechnologies, Polytechnicheskaya, 29, 195251 St. Petersburg, Russia

<sup>°</sup>St. Petersburg State University, Institute of Earth Sciences and <sup>‡</sup>Biology Department, University emb. 7/9, 199034, St. Petersburg, Russia

<sup>´</sup>Becker & Hickl GmbH, Nahmitzer Damm 30, 12277, Berlin, Germany

**KEYWORDS** *Platinum complexes, stimuli responsive phosphorescence, histidine, peptides, proteins, selective covalent conjugation, FLIM/PLIM imaging*

**ABSTRACT:** In this study we have shown that substitution of chloride ligand for imidazole (**Im**) ring in cyclometalated platinum complex, Pt(phpy)(PPh<sub>3</sub>)Cl (**1**; phpy = 2-phenylpyridine; PPh<sub>3</sub> = triphenylphosphine), which is non-emissive in solution, switches on phosphorescence of the resulting compound. Crystallographic and NMR spectroscopic studies of the substitution product showed that the luminescence ignition is a result of **Im** coordination to give the [Pt(phpy)(**Im**)(PPh<sub>3</sub>)]Cl complex. The other imidazole-containing biomolecules such as histidine and histidine-containing peptides and proteins also trigger luminescence of the substitution products. The complex **1** proved to be highly selective towards the imidazole ring coordination that allows site-specific labelling of peptides and proteins with **1** using the route, which is orthogonal to the common bioconjugation schemes *via* lysine, aspartic/glutamic acids or cysteine and does not require any preliminary modification of a biomolecule. The utility of this approach was demonstrated on i) site-specific modification of the ubiquitin – a small protein that contains only one **His** residue in its sequence, and ii) preparation of nonaggregated HSA-based Pt phosphorescent probe. The latter particles easily internalize into the live HeLa cells and display high potential for live cell phosphorescence lifetime imaging (PLIM) as well as for advanced correlation PLIM/FLIM experiments.

## INTRODUCTION

Recent years have seen rapid growth in implementation of phosphorescent metal complexes into bioimaging<sup>1-4</sup> and biosensing.<sup>5-7</sup> This progress is mainly determined by the unique photophysical properties of these lumino-phores: they exhibit enhanced photostability,<sup>8</sup> large Stokes shifts (from 100 to 400 nm)<sup>2</sup> and long excited state lifetimes (µs to ms),<sup>2</sup> the latter makes possible complete signal discrimination from short-lived background fluorescence through spectral<sup>9,10</sup> or temporal<sup>11</sup> resolution. One of the challenges in this area is development of stimuli-responsive probes demonstrating highly selective lumi-

nescence “switching on” in the presence of a specific biomolecule(s). In this context, cyclometalated platinum complexes are among the most advanced “switch on” phosphors because of their square-planar configuration providing high sensitivity to subtle environmental changes. As a result, these compounds are successfully used as DNA sensors and protein stains.<sup>7,12-15</sup>

Nevertheless, currently available cyclometalated platinum “switch on” probes lack binding regioselectivity, which stems from noncovalent mode of their interaction with biomolecules.<sup>7,12-15</sup> For instance, cyclometalated platinum “switch on” probes for DNA are either intercalators

or minor groove binders.<sup>7</sup> In these systems, selectivity is achieved either via selective recognition of some specific DNA structures such as G-quadruplex,<sup>16,17</sup> or via using the aptamers that form double helix exclusively in the presence of the analyte molecule specifically recognized by the aptamer.<sup>7,18</sup> In the case of proteins, “switch on” probes are typically incorporated into their hydrophobic cavities (“pockets”), the way that does not provide substantial regioselectivity and also makes binding reversible with the tendency to dissociate upon high dilution.<sup>12–15</sup> In recent publications<sup>19–21</sup> it was found that Ru(II) diimine and Ir(III) cyclometalated complexes display luminescence “switch on” upon interaction with histidine with superior selectivity of the response over other natural amino acids. However, the authors did not study the chemical details of the complex-histidine interaction having limited it to ESI mass-spectroscopic investigation, based on which the authors of earliest publication<sup>19</sup> even concluded that there is no covalent interaction between histidine and Ru ion.

We believe that alternative binding mechanism, namely formation of covalent/coordination bonds, plays a key role in emission “switching on” and provide the resulting high regioselectivity and enhanced stability of the complexes with histidine and histidine containing biomolecules. Indeed, many types of Pt complexes,<sup>22–24</sup> including anti-tumor drugs,<sup>25–27</sup> are prone to forming coordination bonds with different biomolecules, particularly, with proteins, but there is no reports, which would describe luminescence “switching on” as a result of this process. Another important issue is regioselectivity of binding: Pt compounds typically form complexes with various side groups in proteins that results in nonselective binding.<sup>23,28</sup> Consequently, the development of cyclometalated platinum complexes that could “switch on” their luminescence upon selective binding with some specific groups in biomolecules is strongly desired. In this respect it is also worth noting that histidine-rich proteins play a very important role in many biological processes<sup>29–33</sup> that makes their

detection and monitoring of their presence in tissues and biological media of particular interest.

In this communication, we describe the first, to the best of our knowledge, example of luminescence “switching on” in cyclometalated platinum complex as a result of coordination bond formation with imidazole ring or with biomolecules, which contain this group in their structure, i.e. histidine (**His**) and histidine-containing peptides and proteins. We also show that this binding is highly selective and dominates over interaction with any other amino acid residues present in proteins. This unique feature provides a novel route to site-specific labeling of peptides and proteins as demonstrated by regioselective probe insertion into ubiquitin – the protein that contains only one **His** residue in its amino acid sequence. As a further development of this approach, preparation of nonaggregated HSA-based Pt phosphorescent probe is also demonstrated. This probe easily internalizes into live HeLa cells and displays high potential for recently emerged simultaneous fluorescence/phosphorescence lifetime imaging (FLIM/PLIM)<sup>34,35</sup> of live bio-objects.

## RESULTS AND DISCUSSION

The information concerning interaction of *stimuli responsive* Ir(III)<sup>20,21</sup> and Ru(III)<sup>19</sup> probes with histidine and histidine containing biomolecules indicated that luminescence switch on of the starting non-emissive complexes is due to their interaction with imidazole functionality of histidine to give imidazole substituted compounds, which display considerable emission enhancement compared to the parent complexes. However, none of these communications reported the details of this chemistry and its relation to the photophysical characteristics of the resulting luminescent complexes. Our nearly accidental findings that well known platinum complex Pt<sup>II</sup>(phpy)(PPh<sub>3</sub>)Cl (**1**; where phpy = 2-phenylpyridine; PPh<sub>3</sub> = triphenylphosphine) demonstrates emission “ignition” upon interaction with **HSA** (human serum albumin) prompted

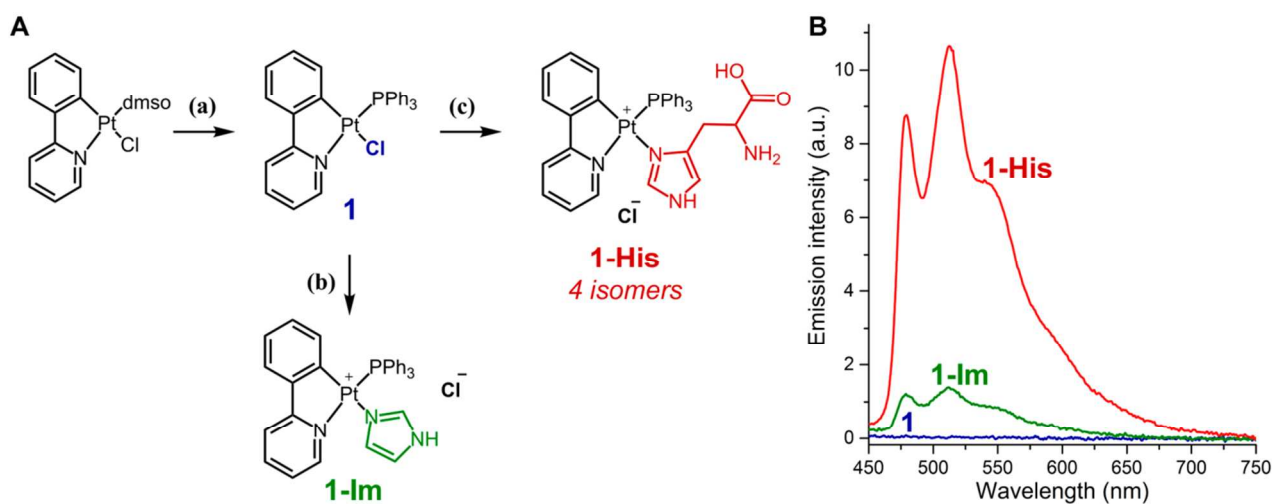


**Figure 1.** Synthesis of complexes **1**, **1-Im** and **1-His**. **A.** Synthetic scheme. Conditions: (a) PPh<sub>3</sub>, CH<sub>2</sub>Cl<sub>2</sub>/Hexane, 4°C; (b) CH<sub>2</sub>Cl<sub>2</sub>, Imidazole (3 equiv), 25°C, 30 min; (c) DMSO/H<sub>2</sub>O, 25°C. **B.** Emission spectra of **1** and mixtures of **1** with 5 equivalents of imidazole (**1-Im**) or histidine (**1-His**); [**1**] = 0.4 mM; solvent - DMSO; λ<sub>ex</sub> = 350 nm.

us to perform detailed investigation of coordination chemistry and photophysics of **1** with imidazole (**Im**) and imidazole containing derivatives, including such biomolecules as ubiquitin and **HSA**. This study clearly indicates that the platinum ion coordination to **Im** functionality plays a key role in the phenomena observed and demonstrated high potential of the suggested approach to regioselective labeling of histidine containing biomolecules and application of **1** in *stimuli responsive* bioimaging.

The complex **1** has been already reported in the article devoted to investigation of anticancer activity of cyclometalated platinum(II) complexes.<sup>36</sup> However, this study describes rather scanty analysis (limited to IR and <sup>1</sup>H NMR spectroscopies) of its structure and stereochemistry and does not contain any information on its reactivity and photophysical properties. Therefore we prepared **1** by reaction of triphenylphosphine with the [Pt(2-phenylpyridine)dmsocI] precursor in dichloromethane/hexane mixture (Figure 1, A) and performed its exhaustive structural characterization. Complex **1** demonstrates polymorphism in solid state: it forms two types of crystals with different unit cell parameters (Table S1). The XRD study of the both polymorphs showed that **1** (Figures 2, A and S1) displays square-planar geometry typical for cyclometalated Pt(II) complexes with the structural parameters in the range typical for this type of platinum compounds. The chloride ligand occupies *cis*-position to the nitrogen atom of the metallocycle, whereas the phosphine ligand was found in *trans*-position.

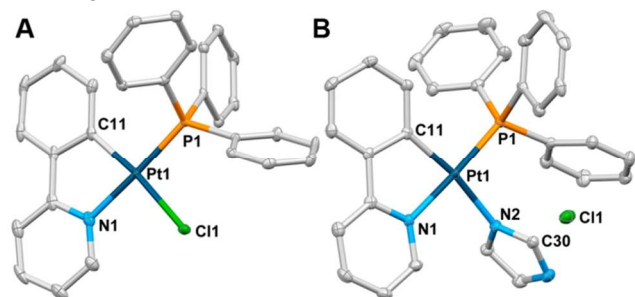


**Figure 2.** Solid-state structure of **1a** (A) and **1-Im** (B). A. Complex **1a**. Selected bond distances (Å): Pt1–C11 2.004(3), Pt1–N1 2.085(3), Pt1–P1 2.2250(1), Pt1–Cl1 2.376(1). Selected angles (°): C11–Pt1–P1 95.38(9), C11–Pt1–N1 80.4(1), N1–Pt1–Cl1 92.60(8), Cl1–Pt1–P1 91.54(3). B. Complex **1-Im**. Selected bond distances (Å): Pt1–C11 2.013(3), Pt1–N1 2.096(2), Pt1–N2 2.101(2), Pt1–P1 2.2377(9). Selected angles (°): C11–Pt1–P1 95.9(1), C11–Pt1–N1 80.5(1), N1–Pt1–N2 91.3(1), N2–Pt1–P1 92.36(7), N1–Pt1–N2–C30 100.4(3). Hydrogen atoms are omitted for clarity.

Combination of the <sup>1</sup>H–<sup>1</sup>H COSY (Figure S2) and <sup>31</sup>P NMR spectra (Figure S3), as well as ESI<sup>+</sup> mass spectrometric data (Figure S4) indicate that **1** retains the same structure in solution.

The complex **1** readily reacts with imidazole and imidazole-containing molecules, e.g. histidine, to give substituted cationic complexes **1-X** (**X** = **Im** or **His**), the latter being soluble in water. The ESI<sup>+</sup> mass-spectrum of the

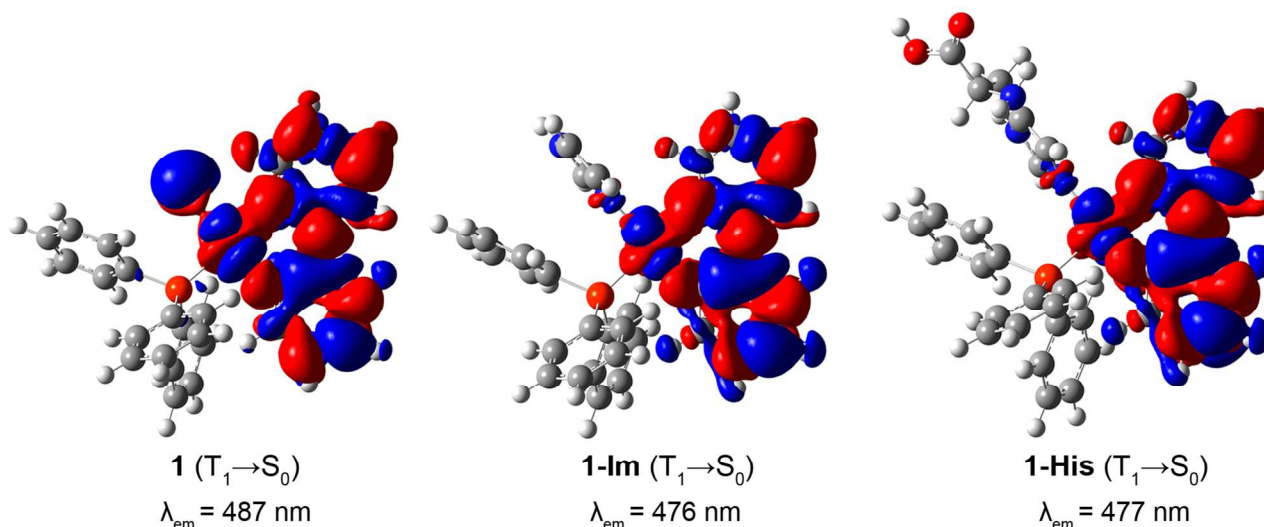
product shows the dominating signal (**[1-Cl+Im]**<sup>+</sup> = 679.1624 m/z) that corresponds to the substitution of the chloride ligand with the imidazole (Figure S5). Similarly, mixing of **1** with histidine results in appearance of the related **[1-Cl+His]**<sup>+</sup> (766.19 m/z) ion in the ESI<sup>+</sup> mass-spectrum that is indicative of a similar chloride ion substitution for histidine (Figure S6). Reaction of **1** with both imidazole and histidine is reversible with rather high equilibrium concentrations of initial compounds; consequently, 3-5-fold excess of imidazole-containing reagents is needed to shift the equilibrium to the right (Figure S7). The imidazole substituted complex **1-Im** easily forms well-defined crystals, while **1-His** does not give single crystals suitable for XRD analysis. The solid state structure of **1-Im** ([Pt(phpy)(PPh<sub>3</sub>)(Im)]Cl) determined by single crystal X-ray crystallography (Figure 2) revealed that it retains square-planar geometry completely analogous to that of **1** with the chloride and phosphine ligands in *cis*- and *trans*-positions to the nitrogen atoms of the metallated ring, respectively. Imidazole coordinates to the platinum ion *via* the N-center bearing free electron pair to give cationic species with the chloride ion in the outer sphere of the complex. The study of **1-Im** using the <sup>1</sup>H–<sup>1</sup>H COSY (Figure S8) and <sup>31</sup>P NMR (Figure S3) spectroscopy shows that it retains the same structure in solution.

More sophisticated behavior is characteristic for the **1-His** complex in solution. The ESI<sup>+</sup> mass-spectrum of the (**1:His** = 1:5) reaction mixture displays only one signal (**[1-Cl+His]**<sup>+</sup>) corresponding to the product of chloride for histidine substitution (Figure S6) in addition to the signals of the starting compounds. However, the <sup>31</sup>P NMR spectrum (Figure S3, S7) of the same mixture consists of several signals with relatively close chemical shifts that indicates formation of a few species corresponding to different conformers or isomers of coordinated histidine in the complexes formed. Detailed analysis of the <sup>1</sup>H–<sup>1</sup>H COSY (Figure S9) and the aliphatic region in the <sup>1</sup>H NMR spectrum (Figure S10) revealed the presence of four isomeric species of **1-His**. Figure S10 demonstrates experimental <sup>1</sup>H spectra of histidine C<sup>β</sup>H<sub>2</sub>–C<sup>α</sup>H moiety in **1-His** and simulated spectra of each isomer; the Table S2 shows the main parameters of the simulated spectra. The existence of two isomers can be explained by tautomerism of imidazolium ring,<sup>37</sup> thus both stereo-inequivalent nitrogen atoms may act as donors of electron pair for platinum atom. Each of these isomers in principle can form some conformers with different orientation of amino acid chain with respect to cyclometalated fragment. The influence of sterically bulky phosphine ligand together with intramolecular non-covalent interactions between coordinated histidine and other parts of the molecule slow down interconversion of the conformers and allows distinguishing of four different species in the <sup>31</sup>P and <sup>1</sup>H NMR spectra. Though there are several hypothetical variants of different stabilized conformers to be formed, we would like to avoid extended speculations on this topic, since it is far beyond

**Table 1.** Photophysical properties of **1** and its complexes with imidazole and different imidazole-containing biomolecules in DMSO and water.

Compound	Abs, nm ( $\epsilon \times 10^{-3}$ , M $^{-1}$ cm $^{-1}$ )	Em, nm <sup>a</sup>	Ex, nm <sup>b</sup>	$\tau(\text{aer})^*$ , $\mu\text{s}^{\text{a,b}}$	$\Phi(\text{aer})^*$ , % <sup>a</sup>	$\tau(\text{deg})^*$ , $\mu\text{s}^{\text{a,b}}$	$\Phi(\text{deg})^*$ , % <sup>a</sup>
<b>1</b> in DMSO	278 (17), 285 (17), 314sh (7.9), 327sh (6.4), 380 (2.9)	The compound is not luminescent					
<b>1-Im</b> in DMSO	268 (18), 276 (18), 296sh (8.1), 316 (6.5), 327 (6.3), 362 (2.8)	477, 510, 538sh	311sh, 340sh, 360	0.5 $\pm$ 0.1	0.17 $\pm$ 0.03	0.8 $\pm$ 0.1	0.23 $\pm$ 0.05
<b>1-His</b> in DMSO	275 (22), 300sh (10.3), 316 (8.5), 327 (8.0), 362 (3.3)	478, 511, 540sh	283, 318sh, 326, 360	0.8 $\pm$ 0.1	0.8 $\pm$ 0.2	1.4 $\pm$ 0.1	1.1 $\pm$ 0.2
<b>1-His</b> in H <sub>2</sub> O	267 (24), 312 (8.1), 322 (7.6), 353 (3.4)	477, 509, 538sh	282, 320, 355	0.8 $\pm$ 0.1	0.36 $\pm$ 0.08	1.9 $\pm$ 0.2	0.5 $\pm$ 0.1
<b>1-Ubq</b> in H <sub>2</sub> O	272 (10), 296sh (3.8), 316 (3.0), 326 (2.7), 360 (1.1)	478, 511, 539sh	275, 317, 326, 360	0.8 $\pm$ 0.1	1.1 $\pm$ 0.2	1.4 $\pm$ 0.1	2.0 $\pm$ 0.4
<b>1-HSA</b> in H <sub>2</sub> O	277 (41), 312sh (4.5), 326sh (3.8), 360sh (1.8)	477, 510, 538sh	275, 316, 327, 360	15.6 $\pm$ 2	15 $\pm$ 3	20.0 $\pm$ 2	18 $\pm$ 4

<sup>a</sup> Excitation wavelength 350 nm; <sup>b</sup> Emission wavelength 510 nm; \*aer/deg – aerated/degassed solution.

**Figure 3.** Electron density difference plots for the lowest energy triplet emission ( $T_1 \rightarrow S_0$ ) of the complexes **1**, **1-Im** and **1-His**. During the electronic transition, the electron density increases in the blue areas and decreases in the red areas. The emission wavelength was estimated from the total energy difference of the optimized states.

of the scope of the present paper. It is also very probable that isomerization described above prevents formation of single crystals suitable for XRD analysis.

Interaction of **1** with compounds containing imidazole ring is not unexpected: binding with histidine via imidazole function has been documented for different platinum complexes,<sup>22,38,39</sup> including those with terpyridine ligand,<sup>40</sup> and cyclometalated Pt(C<sup>N</sup>) complexes.<sup>24,41</sup> However, to the best of our knowledge, none of the above reports have mentioned luminescence ignition as a result of imidazole ring coordination. In the present study, we showed that the most notable feature accompanying coordination of imidazole containing ligands to the cyclometalated Pt(II)

center is switching on the complex luminescence. The complex **1** reveals detectable green luminescence only in solid state (Table S3) but does not display any emission in solution. On the contrary, addition of imidazole or histidine to the solution of **1** gives rise to green luminescence within less than 5 minutes that is necessary to yield appreciable amount of the substituted product (Figure 1, B). Photophysical properties of **1** and its substitution products with imidazole and histidine are summarized in Table 1. All reaction products of **1** with imidazole and imidazole containing biomolecules display nearly identical emission bands (Fig. S11, B) that indicates origin of emission from the same chromophoric center, evidently from

1 the {Pt(C<sup>^</sup>N)} moiety.<sup>42</sup> Both excitation and emission  
2 bands fall into expectable wavelength ranges observed for  
3 the other cyclometalated Pt(C<sup>^</sup>N) complexes.<sup>42</sup> These  
4 observations, together with large Stokes shift, lifetimes in  
5 microsecond domain and clearly resolved vibrational  
6 spacing of ca. 1360 cm<sup>-1</sup> point to IL/MLCT phosphores-  
7 cence typical for this class of platinum complexes.<sup>42</sup>

8 To shed light onto the reasons of the observed lumines-  
9 cence ignition as well as on the nature of electronic tran-  
10 sitions in **1**, **1-Im** and **1-His**, we performed comparative  
11 DFT and TD DFT calculations for these complexes. Re-  
12 sults of calculations (Figure 3 and Figures S12, S13) show  
13 that for all these complexes the nature/composition of  
14 LUMO and HSOMO (Highest Singly Occupied Molecular  
15 Orbital in triplet state) as well as HOMO and LSOMO  
16 (Lowest Singly Occupied Molecular Orbital in triplet  
17 state) are essentially similar. Comparative analysis of the  
18 boundary orbitals in **1**, **1-Im** and **1-His**, however, shows  
19 that LUMO (HSOMO) in these complexes are similar in  
20 nature, but there is a substantial difference between  
21 HOMO (LSOMO). In the case of **1**, the Cl and Pt orbitals  
22 significantly contribute to HOMO (LSOMO) and the con-  
23 tribution of Pt seems to dominate over that of cyclomet-  
24 alated ligand, resulting in a mixed interligand and metal-  
25 to-ligand transition in the case of low energy excitation.  
26 On the contrary, in **1-Im** and **1-His** both HOMO  
27 (LSOMO) and LUMO (HSOMO) are localized at the cy-  
28 clometalated ligand, with slightly smaller contribution of  
29 Pt centered orbitals and without any significant contribu-  
30 tion of imidazole ligands into the orbitals responsible for  
31 emission. This means that emissive transitions in the  
32 complexes containing coordinated imidazole moiety are  
33 of almost pure  $\pi-\pi^*$  intraligand nature perturbed by the  
34 heavy atom effect. Moreover, it was also shown<sup>1-4</sup> that  
35 substitution of chloride with strong field ligands (like  
36 imidazole) results in the growth of the dd excited states  
37 energy, which plays a key role in non-radiative deactiva-  
38 tion of excited states in the Pt(II) complexes of this type,  
39 thus eliminating an important channel of emission  
40 quenching. We believe that both these reasons signifi-  
41 cantly change photophysical behavior of **1-Im** and **1-His**  
42 compared to that of **1** and result in luminescence ignition  
43 in the imidazole containing complexes.

44 The only examples of closely related behavior are Ru(II)  
45 diimine<sup>19</sup> and Ir(III) cyclometalated<sup>20,21</sup> complexes, but in  
46 the Pt(II) chemistry there are no direct analogs of the  
47 complexes presented in this study. Somewhat similar ex-  
48 amples of luminescence “ignition” upon interaction with  
49 biomolecules are: i) a number of “switch-on” Pt probes,<sup>12-15</sup>  
50 which nonselectively stain proteins; such complexes react  
51 with proteins *via* non-covalent (presumably, van-der-  
52 Waals) interactions and thus demonstrate preferable  
53 binding to plasma transport proteins (e.g. serum album-  
54 ins), which possess well-developed hydrophobic cavi-  
55 ties; ii) cyclometalated Pt complex binding to two histi-  
56 dine residues in an amyloid peptide.<sup>24,41</sup> Nevertheless, to  
57 the best of our knowledge, luminescence ignition of Pt(II)

complex resulting from its interaction with  
(bio)molecules containing imidazole ring was not previ-  
ously described.

From the above data on the interaction of **1** with imid-  
azole and histidine, one can anticipate a similar lumines-  
cence switch on upon reaction of **1** with the biomolecules  
containing imidazole ring or histidine, such as histidine  
containing peptides and proteins. This perspective may  
open an avenue for application of **1** in regioselective label-  
ing of these biomolecules accompanied by luminescence  
of the conjugated platinum complex. To date, main bio-  
conjugation strategies involved linking of the luminescent  
probes *via* amino or carboxylic functions presented in  
peptides or proteins ( $\epsilon$ -amino groups of lysine or N-  
terminal amino groups, side groups of aspartic or glutam-  
ic acids or C-terminal carboxylic groups).<sup>43</sup> The probes  
can be involved in one-step conjugation with the above  
residues (e.g. *via* carbodiimide chemistry, using active  
esters, iso(thio)cyanates, aldehydes, etc.); these strategies  
seem to be the most used ones.<sup>43</sup> Alternatively, the same  
residues can be modified to introduce some reactive func-  
tionalities enabling further modification by the probe *via*  
various “bioorthogonal” chemistries (for example, alkynyl  
or azide groups for “click” chemistry<sup>44,45</sup> or aldehyde or  
keto groups for chemical ligation<sup>46,47</sup>); these approaches  
typically provide very fast conjugation with high yields  
but require preliminary modification of biomolecules.  
Ultimately, all the above conjugation strategies involve  
modification of Lys, Glu and Asp residues; however, be-  
cause these residues are the most abundant ones in the  
biomolecules, these approaches are not regioselective.  
Examples of regioselective conjugations are very rare and  
usually limited to peptides rather than to proteins; in the  
latter case, only few examples are reported: i) modifica-  
tion of human serum albumin (**HSA**) *via* free thiol group  
of cysteine-34 using thiol-maleimide click chemistry<sup>48</sup> ii)  
selective oxidation of N-terminal serine leading to genera-  
tion of aldehyde group suitable for oxime and hydrazone  
ligations;<sup>47</sup> iii) selective modification of tryptophan.<sup>49</sup>  
Note that at least two cases (free thiol groups of cysteine  
and N-terminal serine residues) are not typical for pro-  
teins; therefore, there is a strong need in alternative bio-  
conjugation approaches.

In this respect, coordination of **1** to imidazole function  
in histidine seems to be an alternative to standard biocon-  
jugation routes and, contrary to click chemistry or chemi-  
cal ligation approaches, does not require any pre-  
modification of a protein. Moreover, in some cases this  
reaction can provide true regioselective labeling. To evalu-  
ate selectivity of **1** towards different amino acids, we  
added its solution in DMSO to the water solutions of all  
20 natural amino acids and run the mass spectra of the  
mixtures obtained along with monitoring of luminescence  
appearance. We have found that formation of conjugates  
and luminescence ignition were observed in the case of  
histidine, arginine and cysteine (Figure 4, A). However,

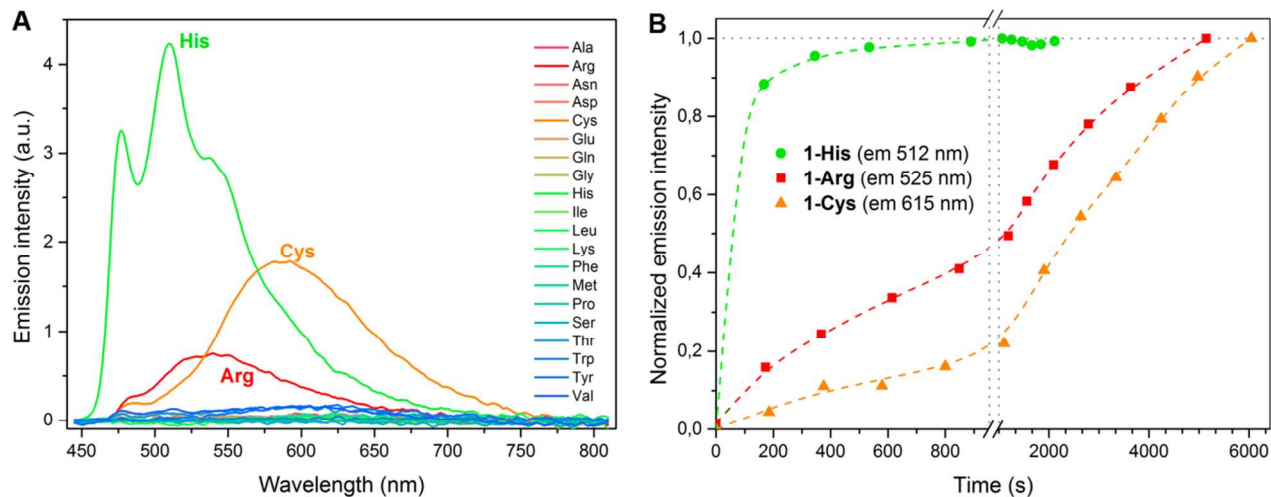


**Figure 4.** A. Emission spectra of **1** (50 μM) in water: DMSO mixture (20 : 1) with 20 natural amino acids (150 μM). Excitation wavelength 365 nm. B. Dependence of luminescence ignition of **1** on time in the presence of histidine, arginine and cysteine in water: DMSO mixture (1 : 21). [**1**] : [amino acid] = 1 : 3; [Pt] = 43.5 μM.

emission wavelength of the conjugates are expectedly different due to coordination of the platinum chromophore to aromatic nitrogen, aliphatic nitrogen and sulfur coordination functions, respectively. Kinetic studies revealed that interaction with histidine proceeds quite fast (quantitative yield is achieved within 5 minutes) while reaction with two amino acids mentioned above occurs much slower (Figure 4, B). Moreover, addition of (3+3) equivalents of histidine/arginine mixture to **1** results in generation of luminescence with the maximum at 510 nm, Figure S14 (same as in the case of **1-Im** and **1-His**), which differs significantly from that of **1-Arg** (broad peak at 520-550 nm). These observations suggest that kinetic control of the complex **1** reactions with histidine, arginine and cysteine results in selective binding of the probe to histidine function in biomolecules containing these amino acids.

To demonstrate the potential of **1** in regioselective labeling of proteins, we have chosen ubiquitin (**Ubq**)<sup>50</sup> as a model. This small protein (M.W. 8565 Da) contains only one histidine residue in its sequence (His-68) and thus can be used to monitor site selectivity in labeling with **1**. In the case of ubiquitin, binding of a probe to histidine is of particular importance, since carboxylic and amino groups of the protein cannot be used for labeling because C-terminal carboxylic group of glycine-76 is the primary group involved in ubiquitination while all the lysine residues are the active functionalities in the polyubiquitination process.<sup>51</sup> In this respect, labeling via His-68 is an extremely useful alternative. We have found that addition of **1** solution in DMSO to the aqueous **Ubq** solution results in appearance of a new signal in the MALDI-TOF mass-spectrum ([**Ubq+1-Cl**] = 9176 m/z; Figure S15) that corresponds to the substitution of chloride ion in **1** with **Ubq** molecule. This reaction is accompanied by emergence of green luminescence, with the emission spectrum of **1-Ubq** nearly identical to that of **1-His** and **1-Im** (Table

1 and Figure S11). These observations imply, as in the case of imidazole and histidine, direct coordination of **Ubq** to Pt ion through imidazole ring of histidine. Moreover, this result also suggests that, despite the presence of four arginine residues in the **Ubq** sequence, interaction of **1** with **Ubq** is highly regioselective towards histidine.

To further prove regioselectivity of this interaction, we performed a comparative 2D NMR study of **1-Ubq** vs **Ubq** using <sup>15</sup>N enriched samples. Figure 5, A shows relative signal loss in the <sup>1</sup>H-<sup>15</sup>N HSQC NMR spectrum of **1-Ubq** compared to that of **Ubq**. The values of relative signal losses were calculated from <sup>1</sup>H-<sup>15</sup>N HSQC spectra, Figure S16, and assigned to each amino acid residue. These experiments made possible to determine the domains, which underwent substantial conformational changes associated with the strongest signal losses. These domains are painted by red color on the amino acid sequence of **Ubq** (upper row in the Figure 5, A) and on the ribbon structures of the protein (Figure 5, B and C). The data obtained indicate that four domains of amino acid sequence show strongest conformational changes: 2-9 (QIFVKTLT), 13-15 (ITL), 44-49 (IFAGKQ), and 65-68 (STLH); these sequences form β-sheets in native form of **Ubq** and are spatially close to each other, the latter one containing histidine residue (Figure 5). Consequently, their simultaneous conformational perturbation detected in the NMR comparative study is most probably caused by coordination of **1** to His-68. As an independent proof of coordination site involved into reaction with **1**, we performed trypsinolysis of **1-Ubq** followed by fingerprint mass-spectrometry analysis of the reaction mixture (Table S4). Both mass spectroscopic signals associated with the presence of platinum complex were associated with the 64-72 (ESTLHLVLR) sequence ([ESTLHLVLR+**1-Cl**] = 1676.705 m/z; [ESTLHLVLR+**1-Cl-TPP**] = 1414.644 m/z). To further localize position of **1** in the sequence 64-72 we

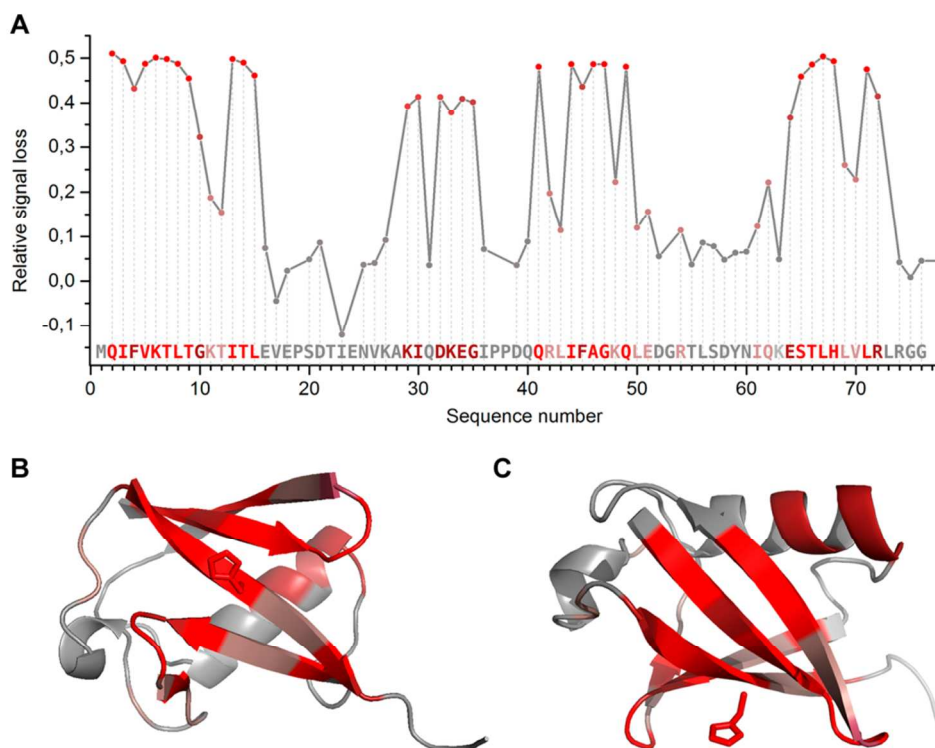


**Figure 5.** Interaction of **1** with ubiquitin. A. Relative signal loss in the  $^1\text{H}$ - $^{15}\text{N}$  HSQC NMR spectra of **1-Ubq** compared to **Ubq** as a function of amino acid sequence. Frontal view (B) and top view (C) of ribbon models of ubiquitin with the color presentation of conformational perturbations. Colors for perturbation degrees: grey - none ( $<0.1$ ); pink - low ( $0.1$ - $0.35$ ); deep pink - medium ( $0.35$ - $0.45$ ); bright red - high ( $>0.45$ ). Number of PDB entry for **Ubq**: 1UBQ. For clarity, the His-68 residue is shown by the red pentagon.

synthesized Ac-ESTLHLVLR-NH<sub>2</sub> peptide, mixed it with **1** and detected new ion that corresponds to the expected conjugate ([peptide+**1**-Cl] = 1717.6 m/z). Finally, the set of data obtained for the reaction of **1** with **Ubq** strongly evidences in favor of the complex binding to **Ubq** via His-68, and makes possible application of **1** for regioselective labeling of histidine-containing peptides and proteins.

Preparation of water-soluble phosphorescent covalent conjugates with functional proteins can be considered as another prospective area of the complex **1** application, provided that the conjugation does not have crucial effect onto the protein functional properties. The assay of the proteinase K (proK) and deoxyribonuclease I (DNase I) activity vs the corresponding conjugates with **1** display negligible effect of conjugation, see SI (Table S6), but extrapolation of these observations onto other proteins/enzymes evidently require additional tests. Human serum albumin (**HSA**), the most abundant human plasma protein, acts as a transporter for a variety of hydrophobic components in human organism. Additionally, **HSA**, being endogenous protein, possesses low systemic toxicity even if conjugated with exogenous molecules, and thus, increases their tolerability.

These considerations prompted us earlier to develop water-soluble **HSA**-based phosphorescent adducts with heterometallic copper subgroup supramolecular clusters that appeared to be applicable in different bioimaging applications, including time-gating<sup>52</sup> and 3D tissue reconstruction by two-photon microscopy.<sup>53</sup> Unfortunately,

further studies have shown that these adducts appear to form aggregates in solution that eventually led to their instability in aqueous media.<sup>53</sup> As a result, the aggregated complexes were not taken up by living cells and imaging experiments could be performed on fixed cells only.<sup>53</sup> The aggregation may be provoked by the presence of rather large polynuclear hydrophobic complexes in the adducts. Taking into account substantially lower size of the mononuclear Pt compounds we performed the synthesis and investigation of covalent **1-HSA** conjugate aiming at overcoming the aggregation drawbacks.

Interaction between **1** and **HSA** proceeds similarly to that between **1** and ubiquitin: addition of **1** to **HSA** leads, on the one hand, to quenching the **HSA** fluorescence (Figure S17, A), and, on the other hand, to appearance of intense green luminescence (Figure S17, A and B). It is worth noting that aggregation properties of **1-HSA** strongly depend on stoichiometry of the reaction mixture: complexes formed at the [1]:[HSA] molar ratios below 1:1 form transparent solutions and do not precipitate under preparative centrifugation at 14,000 rpm and retain their absorbance and luminescence unchanged (ratio Abs(after)/Abs(before) close to 1; Figure 6), while the reaction mixtures with [1]:[HSA] above 1:1 form turbid solutions and give a precipitate under preparative centrifugation (14,000 rpm, 10 min; Figure 6). This finding implies that the conjugates containing one platinum ion per **HSA** molecule are stable to aggregation while further binding

of the platinum complex to available histidine residues leads to the increase in the overall hydrophobicity of the conjugate and to the loss of solubility. Therefore we investigated the properties of **1**-HSA conjugates formed at stoichiometric composition ( $[1]:[HSA] = 1:1$ ) of the reaction mixture. The conjugates are soluble in water; gel permeation chromatography (GPC) reveals both unimers and dimers in the solution of **1**-HSA, and their ratio is shifted towards dimers compared to pure HSA (Figure S18). This proves that aggregation of the conjugates obtained is restricted to dimerization, without formation larger aggregates that would cause precipitation. Although we found that interaction of **1** with the imidazole function is reversible, we observed neither trace amounts of **1** in GPC experiments, nor any loss of absorbance after extensive dialysis (Figure S19). Most probably, the equilibrium which was observed in organic solvents (DMSO) is suppressed in water because of the complex insolubility in aqueous solutions; therefore, the **1**-HSA conjugates are in kinetically 'frozen' state and thus protected from dissociation.

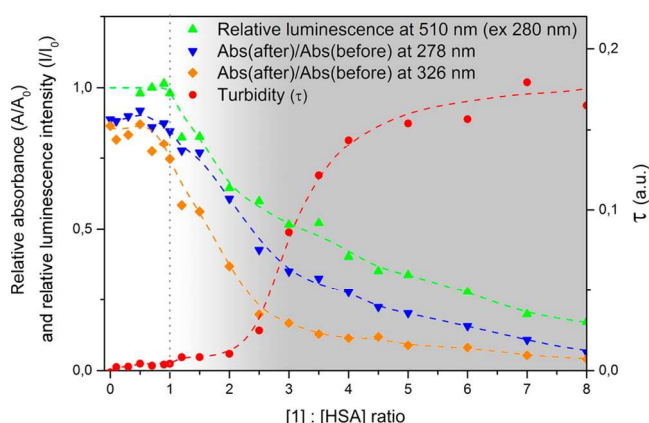


**Figure 6.** UV absorption and luminescence emission ratios after and before centrifugation of **1**-HSA solutions at 14000 rpm, and turbidity ( $\tau = (100-T)/100$ , where  $T$  - solution transmittance, %;<sup>54</sup>) of solution **1**-HSA as a function of  $[1]:[HSA]$  molar ratio. Grayscale filling reflects solution turbidity from transparent (white) to turbid (gray). Vertical dashed line at  $[1]:[HSA] = 1.0$  delineates area of stable solutions ( $[1]:[HSA] \leq 1.0$ ) from area of aggregation instability ( $[1]:[HSA] > 1.0$ ).

The **1**-HSA conjugate demonstrates photophysical characteristics similar to those of **1**-Ubq and **1**-His (Figure S11) but the overall luminescence efficiency is superior compared to those of the other substances: **1**-HSA demonstrates longer lifetimes (12  $\mu$ s) and more than 10-fold increase in quantum yield (Table 1). We believe that both effects stem from more effective shielding of the luminescent center from emission quenching by water and lower vibrational deactivation of the triplet excited state as a result of embedding of **1** into hydrophobic cavities present in the HSA globule.

Long lifetimes of **1**-HSA suggest its applicability in time-resolved bioimaging (e.g. in time-gating<sup>52</sup> or phosphorescent lifetime imaging, PLIM<sup>34</sup>), which benefits from the ability to remove background fluorescence - the

major advantage of phosphors over conventional fluorescent probes. Additionally because the lifetime of the most organometallic phosphorescent complexes depends strongly on the cell microenvironment<sup>11,55,56</sup>, PLIM is also an appropriate technique to analyse the physiological status of living cells and tissues. This is achieved through the environment effects on the kinetics of the probe excited state deactivation that are difficult to measure via steady-state methods. To demonstrate these benefits, we performed recently developed simultaneous phosphorescence/fluorescence lifetime imaging (PLIM/FLIM)<sup>34</sup>. This variant of lifetime-based imaging offers simultaneous mapping of the cell metabolic components having autofluorescence by FLIM and phosphorescent probe distribution in the cell by PLIM. The correlation between metabolic activity, redox ratio and fluorescence lifetime during stem cell differentiation, neurodegenerative diseases, and carcinogenesis was earlier described<sup>57-60</sup>. In particular, it has been shown that the fluorescence lifetime of the coenzyme NAD(P)H (nicotinamide adenine dinucleotide (phosphate)) varies depending on the physiological state of the sample<sup>61-67</sup>. Therefore, in this study the metabolic information is derived from the FLIM data for NAD(P)H. The simultaneous FLIM of NAD(P)H and PLIM of **1**-HSA makes it possible to evaluate the cell microenvironment effect on the **1**-HSA phosphorescence, as well as the **1**-HSA effect on the cells metabolism.<sup>34</sup> The simultaneous FLIM of NAD(P)H and PLIM of **1**-HSA were used for the analysis of live HeLa cells (Figure 7).

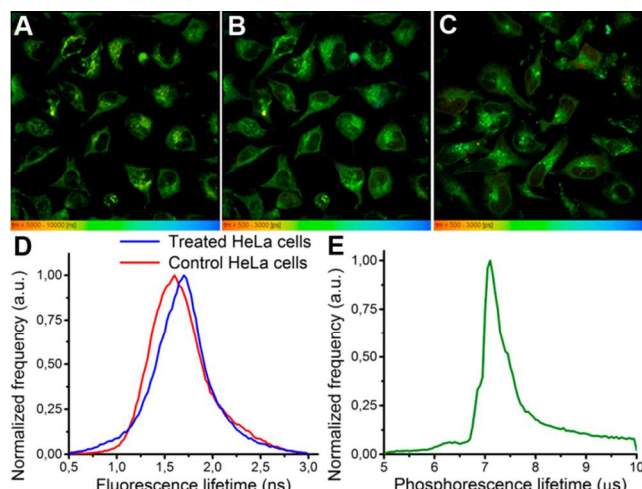


**Figure 7.** Simultaneous FLIM of NAD(P)H and PLIM of **1**-HSA on live HeLa cells. (A) **1**-HSA phosphorescence lifetime imaging of experimental cells treated with **1**-HSA; (B) NAD(P)H fluorescence lifetime imaging of experimental cells treated with **1**-HSA; (C) NAD(P)H fluorescence lifetime imaging of control (nontreated) cells; (D) distribution of NAD(P)H fluorescence lifetimes across the image in experimental (treated with **1**-HSA) and control (nontreated) cells; (E) distribution of **1**-HSA phosphorescence lifetime across the image in experimental cells treated with **1**-HSA.

The **1**-HSA complex in a concentration of 0.3 mg/ml was successfully internalized into live cells and distributed in cytoplasm (Figure 7A). The NAD(P)H lifetime distribution did not change when the cells were incubated

with **1-HSA** as indicated by the comparison of NAD(P)H fluorescence lifetime distributions in experimental and control cells (Figure 7D) while the average NAD(P)H lifetimes in the experimental and control cells were  $1.72 \pm 0.09$  and  $1.68 \pm 0.08$  ns, respectively. The percentage of the free and protein-bound NAD(P)H as well as its fluorescence lifetime remained virtually unchanged in the cells incubated with **1-HSA** (Table S5) that indicates nearly no effect of the conjugate on the cell metabolism. The average phosphorescence lifetime of **1-HSA** in the live cells was  $7.24 \mu\text{s}$  and varies in the  $6.8$  to  $7.8 \mu\text{s}$  range across the image depending on the microenvironment (Figure 7E). Luminescent platinum complexes can be successfully used as oxygen sensors, in particular in the biological and medical studies<sup>11,55,56,68-73</sup> due to their phosphorescence quenching by oxygen. Recently, platinum phosphorescent probes have been adapted for the oxygen measurements in cell cultures<sup>11,56,70,71,74-77</sup>, particularly in microbioreactors<sup>72</sup>, and *in vivo* tissue and organ analysis<sup>69,73,78</sup>. The results clearly show that the **1-HSA** probe retains its long lifetime in biological microenvironment and therefore is amenable for different time-resolved imaging applications, in particular in the simultaneous PLIM/FLIM experiments due to a simple route to preparation, effective internalization into live cells, the absence of effect on cell metabolism and high sensitivity to microenvironment.

## CONCLUSIONS

In conclusion, this study presents the first example of luminescence ignition resulting from chloride ligand substitution with imidazole ring in the platinum cyclometalated complex, Pt(phpy)(PPh<sub>3</sub>)Cl (**1**). The observed effect encompasses various imidazole-containing biomolecules such as histidine and histidine-containing peptides and proteins. The complex **1** displays an extremely high selectivity towards coordination of imidazole ring, which is dictated by both thermodynamics and kinetics of the substitution reaction. This unique feature allows for site-specific labeling of peptides and proteins using **1** with the route that is orthogonal to classic bioconjugation schemes *via* lysine, aspartic/glutamic acids or cysteine and does not require any preliminary modification of a biomolecule. This approach has been tested on the site-specific modification of ubiquitin (a small protein that contains only one His residue in its sequence), and preparation of nonaggregated HSA-based phosphorescent probe applicable for live cell lifetime imaging in the FLIM/PLIM experiments.

## EXPERIMENTAL SECTION

**Materials and Reagents.** 2-Phenylpyridine, triphenylphosphine, imidazole, L-histidine, were obtained from Sigma-Aldrich (USA) and Alfa Aesar (Great Britain). Human serum albumin (HSA) and Recombinant Human Ubiquitin (Ubq) were purchased from Sigma-Aldrich (USA) and Boston Biochem (USA), respectively. The expression and purification procedure for human <sup>15</sup>N uniformly labeled ubiquitin was adapted from the work by Lazar et al.<sup>79</sup> <sup>15</sup>N-ammonium chloride was purchased from

Cambridge Isotope Laboratories. All salts and acids used for preparation of buffer solutions were produced by "Vekton" (Russia) and had analytical-grade purity. The platinum(II) precursor [Pt(2-phenylpyridine)dmsocl] was prepared according to the published procedure<sup>80</sup> by the reaction of potassium tetrachloroplatinate and 2-phenylpyridine in water/2-ethoxyethanol solution followed by heating at 80 °C in DMSO for 48 hours. Dichloromethane was purified and distilled using standard procedure. Water was purified using Simplicity Water Purification System Merck Millipore (type 1 water).

**Instrumentation.** Solution <sup>1</sup>H NMR, <sup>1</sup>H-<sup>1</sup>H COSY, and <sup>31</sup>P NMR spectra were recorded with a Bruker Avance III (400 MHz) and a Bruker Avance III (500 MHz) spectrometers (Bruker, Germany). Simulation of the <sup>1</sup>H spectra was performed using Dr. Kirk Marat SpinWorks (Canada)<sup>81</sup> and Bruker NMRsim programs. The ESI<sup>+</sup> mass spectra were obtained with a MaXis instrument (Bruker, Germany), in the ESI<sup>+</sup> mode (solvent MeOH). Microanalyses were carried out with a Euro EA-3028HT Elemental Analyzer (EuroVector, Italy). Gel permeation chromatography (GPC) was performed with high performance liquid chromatograph Shimadzu LC-20 Prominence (Shimadzu, Japan) equipped with RF-20A and SDD-M20A detectors and PSS PROTEEMA 300 column. Microcrystalline samples were used for the photophysical experiments in the solid state. Steady-state photoluminescence spectra were recorded on a Fluorolog-3 (JY Horiba Inc., Japan) spectrofluorimeter. Lifetimes measurements in solid state were carried out with the Time-Correlated Single Photon Counting (TCSPC) method and the results have been treated with the Jobin-Yvon software package and the Origin 8.1 program. Direct quantum yield measurements for the crystalline samples were performed at room temperature with an integrating sphere from Quanta-phi (JY Horiba Inc., Japan). UV/Vis spectra and turbidity measurements were recorded with a Shimadzu UV-1800 spectrophotometer. Turbidity ( $\tau$ ) was recalculated from solutions transmittance (T, %):  $\tau = (100-T)/100$ .<sup>54</sup> Emission spectra in solution were recorded on a FluoMax-4 (JY Horiba Inc., Japan) spectrofluorimeter. The pulse laser DTL-399QT (Laser-export Co. Ltd., Russia; 351 nm, 50 mW, pulse width 6 ns, repetition rate 1 kHz), monochromator MUM (LOMO, Russia; bandwidth of slit 1 nm), photon counting head H10682 (Hamamatsu Photonics, Japan) and multiple-event time digitizer P7887 (FAST ComTec GmbH, Germany) were used for lifetime measurements in solution. The absolute emission quantum yield in solution was determined by the comparative method<sup>82</sup> using 9,10-diphenylanthracene in cyclohexane ( $\Phi_r = 0.97$ ) as the reference with the refraction indexes of cyclohexane, DMSO and water equal to 1.426, 1.477 and 1.333 respectively.<sup>83</sup>

**Synthesis of 1.** [Pt(2-phenylpyridine)dmsocl] (100 mg, 0.216mmol) and triphenylphosphine (57 mg, 0.216mmol) were dissolved in 5 ml dichloromethane, then 1 ml hexane was added. Resulting product was obtained as pale yellow crystals by slow evaporation of solvent at 4°C. Yield: 119 mg (85%). <sup>1</sup>H NMR (400 MHz, CDCl<sub>3</sub>, 25 °C):  $\delta = 9.92 -$

9.88 (m with broad  $^{195}\text{Pt}$  satellites,  $^3J_{\text{Pt,H}} = 26.1$  Hz, 1 H<sup>1</sup>), 7.87 (td,  $^3J_{\text{H,H}} = 7.8$ , 1.4 Hz, 1 H<sup>3</sup>), 7.84 – 7.77 (m, 7 H<sup>3,9,4</sup>), 7.52 (d,  $^3J_{\text{H,H}} = 7.5$  Hz, 1 H<sup>5</sup>), 7.43 (td,  $^3J_{\text{H,H}} = 7.3$ , 1.9 Hz, 3 H<sup>11</sup>), 7.37 (td,  $^3J_{\text{H,H}} = 7.8$ , 1.9 Hz, 6 H<sup>10</sup>), 7.29 (dd,  $^3J_{\text{H,H}} = 7.1$ , 6.0 Hz, 1 H<sup>2</sup>), 6.96 (t,  $^3J_{\text{H,H}} = 7.4$  Hz, 1 H<sup>6</sup>), 6.68 (dd with broad  $^{195}\text{Pt}$  satellites,  $^3J_{\text{H,H}} = 7.8$ , 3.2,  $^3J_{\text{Pt,H}} = 55.5$  Hz, 1 H<sup>8</sup>), 6.52 (td,  $^3J_{\text{H,H}} = 7.5$ , 1.0 Hz, 1 H<sup>7</sup>) ppm. Please refer the Supporting Information for proton assignments.  $^1\text{H}$  NMR (400 MHz,  $(\text{CD}_3)_2\text{SO}$ , 25 °C):  $\delta = 9.75 - 9.60$  (m with broad  $^{195}\text{Pt}$  satellites, 1H), 8.21 – 8.11 (m, 2H), 7.75 (d,  $^3J_{\text{H,H}} = 7.3$  Hz, 1H), 7.73 – 7.63 (m, 5H), 7.57 (t,  $^3J_{\text{H,H}} = 6.2$  Hz, 1H), 7.54 – 7.40 (m, 9H), 6.95 (t,  $^3J_{\text{H,H}} = 7.4$  Hz, 1H), 6.54 (dd with broad  $^{195}\text{Pt}$  satellites,  $^3J_{\text{H,H}} = 7.1$ , 3.2 Hz, 1H), 6.48 (t,  $^3J_{\text{H,H}} = 7.4$  Hz, 1H).  $^{31}\text{P}$  NMR (400 MHz,  $(\text{CD}_3)_2\text{SO}$ , 25 °C):  $\delta = 23.41$  (d,  $^1J_{\text{P,Pt}} = 4321.5$  Hz, 1P) ppm. ESI<sup>+</sup>-MS(*m/z*): [M-Cl]<sup>+</sup> found 611.1187, calculated 611.1219, [M+Na]<sup>+</sup> found 669.0760, calculated 669.0805, [2M-Cl]<sup>+</sup> found 1257.2122, calculated 1257.2116. C<sub>29</sub>H<sub>23</sub>CINPPt (647.01): calcd. C 53.83, H 3.58, N 2.16; found C 54.06, H 3.68, N 1.87.

**Synthesis of 1-Im.** Complex **1** (10 mg, 0.015 mmol) was dissolved in  $\text{CH}_2\text{Cl}_2$  (5 ml), then imidazole (3.3 mg, 0.045 mmol) was added. The reaction mixture was stirred at room temperature for 30 min. It was then concentrated to ca. 2 ml under vacuum and layered with ca. 1 ml of hexane. The product was obtained as yellow-green crystals by slow diffusion of hexane into dichloromethane solution at 4 °C. Yield: 10.9 mg (99 %).  $^1\text{H}$  NMR (400 MHz,  $(\text{CD}_3)_2\text{SO}$ , 25 °C):  $\delta = 8.17$  (d,  $^3J_{\text{H,H}} = 8.2$  Hz, 1H<sup>4</sup>), 8.10 (t,  $^3J_{\text{H,H}} = 7.8$  Hz, 1H<sup>3</sup>), 7.78 (s, 1H<sup>12</sup>), 7.74 (d,  $^3J_{\text{H,H}} = 7.8$  Hz, 1H<sup>5</sup>), 7.61 (dd,  $^3J_{\text{H,H}} = 11.9$ , 7.4 Hz, 6H<sup>9</sup>), 7.50 (dd,  $^3J_{\text{H,H}} = 7.8$ , 6.2 Hz, 3H<sup>11</sup>), 7.38 (td,  $^3J_{\text{H,H}} = 7.7$ , 2.2 Hz, 6H<sup>10</sup>), 7.31 (t,  $^3J_{\text{H,H}} = 6.6$  Hz, 1H<sup>2</sup>), 7.23 – 7.15 (m, 1H<sup>1</sup>), 7.03–6.99 (m, 2H<sup>13,6</sup>), 6.92 (s, 1H<sup>4</sup>), 6.56–6.50 (m, 2H<sup>7,8</sup>). Please refer the Supporting Information for proton assignments.  $^{31}\text{P}$  NMR (400 MHz,  $(\text{CD}_3)_2\text{SO}:\text{D}_2\text{O}$  5:1, 25 °C):  $\delta = 22.34$  (d,  $^1J_{\text{P,Pt}} = 4211.1$  Hz, 1P) ppm. ESI<sup>+</sup>-MS(*m/z*): [M-Cl]<sup>+</sup> found 679.1624, calculated 679.1593.

**Synthesis of 1-His.** The complex **1** (2 mg, 0.003 mmol) was dissolved in DMSO-*d*<sub>6</sub> (0.6 ml), and L-histidine (3 mg, 0.019 mmol) was dissolved in 200  $\mu\text{l}$  deuterated water; the concentrations of resulted solutions were 3.33 mg/ml (5.2 mM) and 15 mg/ml (97 mM) respectively. Aliquots of the amino acid solution were added to the solution of **1** in a NMR-tube, and the mixtures were incubated at room temperature for 2 h. The  $^1\text{H}$  and  $^{31}\text{P}$  NMR-spectra were measured for solutions with different {histidine/**1**} ratios (Figure S7).  $^1\text{H}$  NMR (400 MHz,  $(\text{CD}_3)_2\text{SO}:\text{D}_2\text{O} = 10:1$ , 25 °C):  $\delta = 8.20$  (d,  $^3J_{\text{H,H}} = 7.9$  Hz, 1H<sup>4</sup>), 8.12 (t,  $^3J_{\text{H,H}} = 8.5$  Hz, 1H<sup>3</sup>), 7.95 – 7.73 (m, 1H<sup>12</sup>), 7.77 (d,  $J = 7.6$  Hz, 1H<sup>5</sup>), 7.67 – 7.58 (m, 6H<sup>9</sup>), 7.57 – 7.49 (m, 4H<sup>11</sup>), 7.43 – 7.37 (m, 6H<sup>10</sup>), 7.30 (dd,  $^3J_{\text{H,H}} = 13.5$ , 6.4 Hz, 1H<sup>2</sup>), 7.01 (td,  $^3J_{\text{H,H}} = 8.1$ , 3.1 Hz, 1H<sup>6</sup>), 6.96 – 6.59 (m, 1H<sup>13</sup>), 6.54 (m, 2H<sup>7,8</sup>), 3.42 – 3.28 (m, 1H<sup>16</sup>), 3.29 – 2.45 (m, 2H<sup>14,15</sup>). Please refer the Supporting Information for proton assignments.  $^{31}\text{P}$  NMR (400 MHz,  $(\text{CD}_3)_2\text{SO}:\text{D}_2\text{O} = 10:1$ , 25 °C):  $\delta = 22.34 - 22.07$  (m,  $^1J_{\text{P,Pt}} = 4200$  Hz, 1P) ppm. ESI<sup>+</sup>-MS(*m/z*): [M-Cl]<sup>+</sup> found 766.1933, calculated 766.1914.

**Preparation of the 1-HSA and 1-Ubq conjugates.** HSA (32.57 mg, 0.489  $\mu\text{mol}$ ) was dissolved in 1 ml of wa-

ter, and complex **1** (1.45 mg, 2.241  $\mu\text{mol}$ ) was dissolved in DMSO (1.0998 g), the concentrations of resulted solutions were 0.48 mM and 2.24 mM respectively. The complex solution was gradually added portionwise to the protein solution, ultimately 200  $\mu\text{l}$  of complex solution were added. After each addition, the mixture was gently stirred. The mixture was incubated for 1 h, and then 2 ml of water were added. DMSO was removed by dialysis with 6-8 kDa MWCO membrane (Orange Scientific, Belgium) for 24 h at room temperature with 5 water changes. Resulted solution was centrifuged at 4000g for 10 minutes. The sample was lyophilized with freeze dryer. **1-Ubq** was prepared using the same methodology except that 2 kDa MWCO dialysis membranes (Sigma-Aldrich, USA) were used.

**DFT calculations of 1 and 1-Im** The **1**, **1-Im** and **1-His** complexes were performed using the Gaussian 09 program package<sup>84</sup> at the density functional theory level (DFT) with the hybrid density functional B3LYP.<sup>85-87</sup> Platinum atoms were described by Stuttgart-Dresden pseudopotential basis set (SDD)<sup>88</sup> while all electron Pople's basis set 6-311+G\* was used for all other atoms. The geometries of lowest singlet and triplet states were optimized at the above mentioned level of the theory. The excited states of the complexes were studied by time dependent density functional theory (TDDFT) calculations.

**Monitoring of reactions of 1 with amino acids using UV-Vis and emission spectroscopy.** The following stock solutions were prepared: 1 mM solution of complex **1** in DMSO; 3 mM solution of the corresponding amino acid in water. Two milliliters of DMSO, 100  $\mu\text{l}$  of **1** solution and 100  $\mu\text{l}$  of amino acid solution were mixed in 1 cm quartz cuvette. Absorption and emission spectra were taken at a regular time interval starting from the moment as close as possible to the mixing point. The measurements were carried out for histidine, cysteine, arginine and equimolar arginine/histidine mixture.

**NMR experiments with 1-Ubq.** The  $^{15}\text{N}$  labeled **Ubq** stock solution (0.5 mM) was prepared by dissolving of solid protein in 50 mM PBS pH 6.5. The stock solutions of **1** (1.5 mM) were prepared by dissolving of the solid complex (0.77 mg,  $1.2 \times 10^{-6}$  mol) in DMSO-*d*<sub>6</sub> (877 mg). Two probes were prepared — the mixture of the **Ubq** solution and **1** solution (the **Ubq**:**1** ratio was 1:1; the H<sub>2</sub>O:DMSO-*d*<sub>6</sub> ratio was 3:1), and the mixture of the **Ubq** solution and DMSO-*d*<sub>6</sub> (the H<sub>2</sub>O/DMSO-*d*<sub>6</sub> ratio was 3:1). After incubating for 2 hours  $^1\text{H}$ - $^{15}\text{N}$  HSQC NMR spectra were recorded.  $^1\text{H}$ - $^{15}\text{N}$  HSQC spectra were measured on a Bruker AVANCE III spectrometer (500.03 MHz  $^1\text{H}$ , 50.67 MHz  $^{15}\text{N}$ ) at 298 K using 5 mm BBO probehead; the spectra were obtained using standard Bruker “hsqcetf3gp” pulse program.  $^1\text{H}$  and  $^{15}\text{N}$  hard pulse fields were 19.7 and 16.7 kHz, respectively. Spectral widths were 7.0 and 2.8 kHz for the direct  $^1\text{H}$  and indirect  $^{15}\text{N}$  dimensions. The data matrix consisted of 4096 (direct dimension) by 512 (indirect dimension) real data points. Number of acquisitions was 16 (for three hour) or 80 (for overnight measurement). The spectra were processed by NMRPipe<sup>89</sup> and analyzed by NMRDraw<sup>89</sup> and Sparky.<sup>90</sup>

**MALDI mass-spectroscopy of 1-Ubq conjugate.** Mass spectra were recorded by AB SCIEX TOF/TOF 5800 MALDI spectrometer in linear mode. The instrument was calibrated using a Mass Standards Kit for Calibration of AB Sciex TOF/TOF Instruments (AB Sciex). The stock solutions of the samples for MALDI experiments (100  $\mu\text{M}$ ) were prepared by dissolving pure Ubiquitin or lyophilizate of **1-Ubq** conjugate in ultrapure water and dilution with 0.1% trifluoroacetic acid (TFA) (Sigma-Aldrich, USA) up to concentration 10  $\mu\text{M}$ . The samples (0.5  $\mu\text{l}$ ) were spotted onto a steel plate and air-dried at room ambience. Then 0.5  $\mu\text{l}$  of sinapinic acid matrix solution (Sigma-Aldrich, 10 mg/ml in 70% acetonitrile and 0.1% TFA) was spotted on samples and air-dried at room ambience. The accuracy of the mass peak measurements in linear mode was about 5 Da.

**Trypsinolysis of 1-Ubq conjugate and its fingerprint mass-spectroscopy.** The stock solutions of Ubiquitin and **1-Ubq** conjugate were diluted up to concentration 50  $\mu\text{M}$  in the 100 mM ammonium bicarbonate buffer ( $\text{NH}_4\text{HCO}_3$ , Sigma-Aldrich, USA) followed by addition of solution of proteomic grade trypsin (0.2  $\mu\text{g}/\mu\text{l}$  in 50mM  $\text{NH}_4\text{HCO}_3$ , Sigma-Aldrich, USA), 0.2  $\mu\text{g}$  of trypsin per 2  $\mu\text{g}$  of the sample. Solutions were incubated for 4 hours at 37°C, hydrolysis was stopped by adding to sample an equal volume of 0.1% TFA. The samples obtained (0.4  $\mu\text{l}$ ) were spotted on a steel plate with 0.4  $\mu\text{l}$  of a 2,5-dihydroxybenzoic acid matrix (Sigma-Aldrich, USA) and air-dried at room ambience. High-resolution mass spectra were recorded using a Fourier Transform Ion Cyclotron Resonance Mass Spectrometer (Varian 902-MS) equipped by 9.4 T magnet (FTMS) in positive MALDI mode. The instrument was calibrated using ProteoMass Peptide MALDI-MS Calibration Kit (Sigma-Aldrich, USA). The accuracy of the mass peak measurements after recalibration with trypsin autolysis peak (842, 5094 Da) was better than 2 ppm. Analysis of the MS data was carried out with FTDocViewer software (Varian, USA) and identification of peptides was performed using Mascot software (www.matrixscience.com).

**Fluorescent titration of HSA with complex 1.** The HSA stock solution (30  $\mu\text{M}$ ) was prepared by dissolving of solid protein (6.2 mg) in ultrapure water (3.125 g) and stored at room temperature for 24h. The stock solutions of **1** in DMSO (1 mM; 700  $\mu\text{M}$ ; 300  $\mu\text{M}$ ; 100  $\mu\text{M}$ ; 30  $\mu\text{M}$ ) were prepared. The stock solutions of protein and **1** were mixed in appropriate amounts to give a series of 27 mixtures with the HSA:**1** ratio from 1:0 to 1:15. The  $\text{H}_2\text{O}$ :DMSO(18:1) ratio was kept constant for all solutions. Concentration of protein was 1.5  $\mu\text{M}$ ; concentration of platinum complex varied from 0  $\mu\text{M}$  to 22.5  $\mu\text{M}$ . The solutions were incubated for 24h. Then each solution was divided into two parts. One part was centrifuged (10 min, 10000 g) and the other one was investigated without centrifugation. Absorption, emission and excitation spectra were obtained for each solution in 10 mm quartz cuvette.

**Analytical chromatography of 1-HSA.** The **1-HSA** solutions prepared for titration experiment were investigated by analytical gel-permeation chromatography (GPC).

Chromatography was carried out using 10 mM PBS (pH 6.6) as an eluent. The flow rate was 0.5 ml/min.

**Dialysis of 1-HSA.** Solid **1-HSA** (10 mg) was dissolved in 10 ml of water (1 mg/ml, 150  $\mu\text{M}$ ), and an aliquot was taken. The remainder of the solution was placed in dialysis tube (6-8 kDa MWCO membrane). The dialysis was carried out for 6 days and 21 outer solution changes were performed. Aliquots of the **1-HSA** solution were taken periodically and corresponding UV/Vis absorption and luminescence emission spectra were recorded.

**Cell cultures preparation.** La cells were cultivated in F-12 culture medium (PAN-Biotech, Germany) with 10% fetal bovine serum (PAN-Biotech, Germany). Cells were cultivated on  $\mu$ -dishes having a glass bottom (Ibidi, Germany) and on open 8 wells  $\mu$ -slides with a glass bottom (Ibidi, Germany) in  $\text{CO}_2$ -incubator with 5%  $\text{CO}_2$  at 37°C. After 24-hour pre-incubation **1-HSA** was added to experimental cell samples for final concentration of 0.3 mg/ml. **1-HSA** was dissolved in F-12 medium. Culture medium without **1-HSA** was added to control cell samples. After this all samples were cultivated during 24 h under the same conditions. The culture medium was then removed and the cells were rinsed three times with DPBS.

**Simultaneous FLIM of NAD(P)H and PLIM of 1-HSA.** We used Nikon TE 2000 inverted fluorescence microscope (Nikon, Japan) equipped with a confocal scanner DCS-120 and a Simple-Tau 150 time correlated single photon counting (TCSPC) system (Becker and Hickl GmbH, Berlin, Germany) to simultaneously record FLIM of NAD(P)H and PLIM of **1-HSA**. The detailed approach to perform combined PLIM/FLIM has been published earlier.<sup>34,35</sup> 405nm ps laser (BDL-405 SMN, Becker&Hickl GmbH, Berlin, Germany) was used for simultaneous NAD(P)H and **1-HSA** excitation. The fluorescence and the phosphorescence signals were recorded with HPM-100-40 detector (Becker&Hickl GmbH, Berlin, Germany). All images were collected with oil immersion Nikon objective (Nikon S Fluor, 40x, 1.3, Japan). The fluorescence and the phosphorescence signals were separated by a 510 LP dichroic mirror (Chroma, USA). TCSPC data were analyzed by SPCImage 5.4 software (Becker and Hickl GmbH, Berlin, Germany).

## ASSOCIATED CONTENT

**Supporting Information.** The Supporting Information is available free of charge at <http://pubs.acs.org>.

## AUTHOR INFORMATION

### Corresponding Author

\*E-mail: sergey.tunik@spbu.ru; stunik@inbox.ru; Fax: +7 (812) 3241258

## ACKNOWLEDGMENT

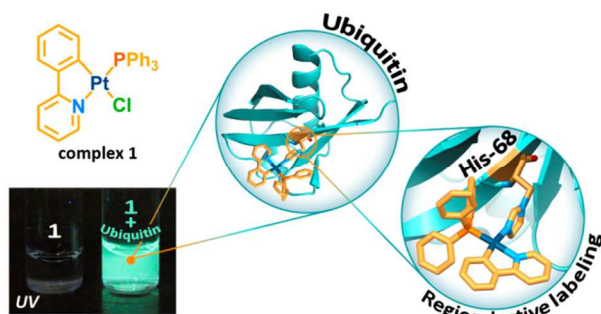
All the research presented in this paper, excluding bioimaging experiments, were supported by Russian Science Foundation, grant No 16-43-03003. The bioimaging study (FLIM/PLIM experiments) has been done with the support from Saint-Petersburg State University research grants No 1.37.153.2014 and No 1.50.1043.2014 using TC SPS system

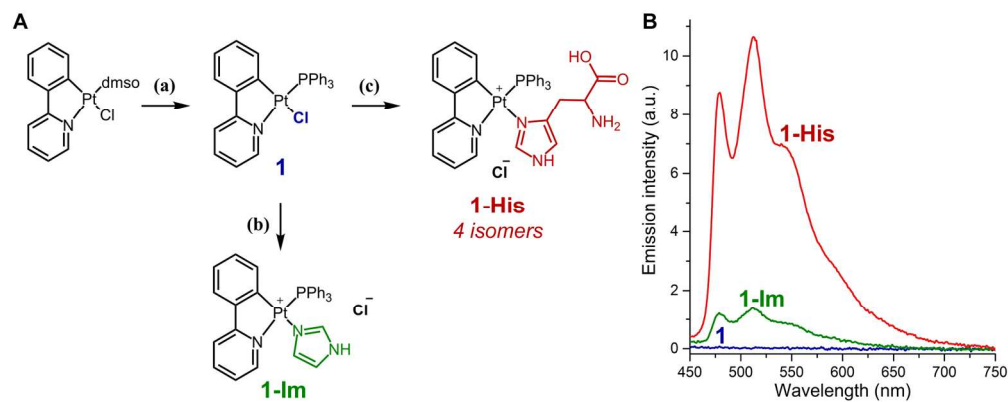
(Becker and Hickl GmbH, Berlin Germany) in the Max Dlebrück Center for Molecular Medicine (Berlin, Germany). The NMR, photophysical, analytical, and crystallographic measurements were performed using the following core facilities at St. Petersburg State University Research Park: Centre for Magnetic Resonance, Centre for Optical and Laser Materials Research, Centre for Chemical Analysis and Materials Research, Computing Centre, and X-ray Diffraction Centre and Chromas Core Facility. Lifetime measurements were carried out using scientific equipment of the analytical center of nano- and biotechnologies of SPbSPU.

## REFERENCES

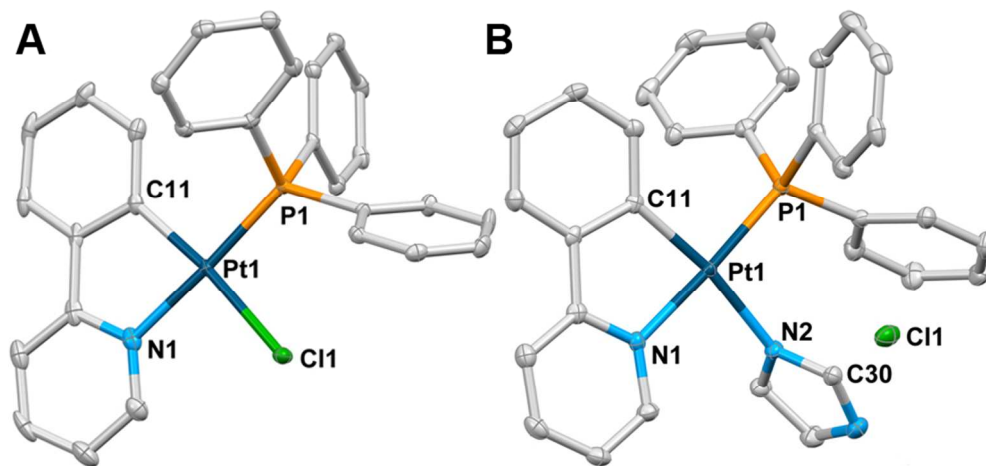
- (1) Fernández-Moreira, V.; Thorp-Greenwood, F. L.; Coogan, M. P. *Chem. Commun.* **2010**, 46 (2), 186–202.
- (2) Zhao, Q.; Huang, C.; Li, F. *Chem. Soc. Rev.* **2011**, 40 (5), 2508–2524.
- (3) Thorp-Greenwood, F. L. *Organometallics* **2012**, 31 (16), 5686–5692.
- (4) Coogan, M. P.; Fernández-Moreira, V. *Chem. Commun.* **2014**, 50 (4), 384–399.
- (5) Demas, J. N.; DeGraff, B. A. *Coord. Chem. Rev.* **2001**, 211 (1), 317–351.
- (6) Lo, K. K.-W.; Choi, A. W.-T.; Law, W. H.-T. *Dalt. Trans.* **2012**, 41 (20), 6021.
- (7) Ma, D.-L.; Ma, V. P.-Y.; Chan, D. S.-H.; Leung, K.-H.; He, H.-Z.; Leung, C.-H. *Coord. Chem. Rev.* **2012**, 256 (23), 3087–3113.
- (8) Yu, M.; Zhao, Q.; Shi, L.; Li, F.; Zhou, Z.; Yang, H.; Yi, T.; Huang, C. *Chem. Commun.* **2008**, 102 (18), 2115.
- (9) Zimmermann, T.; Rietdorf, J.; Pepperkok, R. *FEBS Lett.* **2003**, 546 (1), 87–92.
- (10) Zimmermann, T. In *Microscopy Techniques*; Springer Berlin Heidelberg, 2005; pp 245–265.
- (11) Baggaley, E.; Botchway, S. W.; Haycock, J. W.; Morris, H.; Sazanovich, I. V.; Williams, J. A. G.; Weinstein, J. A. *Chem. Sci.* **2014**, 5 (3), 879–886.
- (12) Kit-Man Siu, P.; Ma, D.-L.; Che, C.-M. *Chem. Commun.* **2005**, 18 (8), 1025–1027.
- (13) Wu, P.; Wong, E. L.-M.; Ma, D.-L.; Tong, G. S.-M.; Ng, K.-M.; Che, C.-M. *Chem. Eur. J.* **2009**, 15 (15), 3652–3656.
- (14) Che, C.-M.; Zhang, J.-L.; Lin, L.-R. *Chem. Commun.* **2002**, 97 (21), 2556–2557.
- (15) Vaidyanathan, V. G.; Nair, B. U. *Eur. J. Inorg. Chem.* **2005**, 2005 (18), 3756–3759.
- (16) Ma, D.-L.; Che, C.-M.; Yan, S.-C. *J. Am. Chem. Soc.* **2009**, 131 (5), 1835–1846.
- (17) Man, B. Y.-W.; Chan, D. S.-H.; Yang, H.; Ang, S.-W.; Yang, F.; Yan, S.-C.; Ho, C.-M.; Wu, P.; Che, C.-M.; Leung, C.-H.; Ma, D.-L. *Chem. Commun.* **2010**, 46 (45), 8534.
- (18) Leung, K.-H.; He, H.-Z.; Chan, D. S.-H.; Fu, W.-C.; Leung, C.-H.; Ma, D.-L. *Sens. Actuators B-Chem.* **2013**, 177, 487–492.
- (19) Wong, C.-Y.; Chung, L.-H.; Lin, S.; Chan, D. S.-H.; Leung, C.-H.; Ma, D.-L. *Sci. Rep.* **2014**, 4, 7136.
- (20) Ma, D.-L.; Wong, W.-L.; Chung, W.-H.; Chan, F.-Y.; So, P.-K.; Lai, T.-S.; Zhou, Z.-Y.; Leung, Y.-C.; Wong, K.-Y. *Angew. Chem. Int. Ed.* **2008**, 47 (20), 3735–3739.
- (21) Li, C.; Yu, M.; Sun, Y.; Wu, Y.; Huang, C.; Li, F. *J. Am. Chem. Soc.* **2011**, 133 (29), 11231–11239.
- (22) Iakovidis, A.; Hadjiliadis, N. *Coord. Chem. Rev.* **1994**, 135, 17–63.
- (23) Espósito, B. P.; Najjar, R. *Coord. Chem. Rev.* **2002**, 232 (1), 137–149.
- (24) Valensin, D.; Gabbiani, C.; Messori, L. *Coord. Chem. Rev.* **2012**, 256 (19), 2357–2366.
- (25) Messori, L.; Marzo, T.; Merlino, A. *J. Inorg. Biochem.* **2015**, 153, 136–142.
- (26) Picone, D.; Donnarumma, F.; Ferraro, G.; Russo Krauss, I.; Fagagnini, A.; Gotte, G.; Merlino, A. *J. Inorg. Biochem.* **2015**, 146, 37–43.
- (27) Ferraro, G.; Massai, L.; Messori, L.; Merlino, A. *Chem. Commun.* **2015**, 51 (46), 9436–9439.
- (28) Ferraro, G.; Massai, L.; Messori, L.; Merlino, A. *Chem. Commun. (Camb)*. **2015**, 51 (46), 9436–9439.
- (29) Sullivan, D. J. J.; Gluzman, L. Y.; Goldberg, D. E. *Science* **1996**, 271 (5246), 219–222.
- (30) Jones, A. L.; Hulett, M. D.; Parish, C. R. *Immunol. Cell Biol.* **2005**, 83 (2), 106–118.
- (31) Engesser, L.; Kluff, C.; Briët, E.; Brommer, E. J. P. *Br. J. Haematol.* **2008**, 67 (3), 355–358.
- (32) Kuhli, C.; Scharrer, I.; Koch, F.; Hattenbach, L.-O. *Am. J. Ophthalmol.* **2003**, 135 (2), 232–234.
- (33) Bartneck, M.; Fech, V.; Ehling, J.; Govaere, O.; Warzecha, K. T.; Hittatiya, K.; Vucur, M.; Gautheron, J.; Luedde, T.; Trautwein, C. et al. *Hepatology* **2016**, 63 (4), 1310–1324.
- (34) Shchslavskiy, V. I.; Neubauer, A.; Bukowiecki, R.; Dinter, F.; Becker, W. *Appl. Phys. Lett.* **2016**, 108 (9), 9111.
- (35) Kalinina, S.; Breymer, J.; Schäfer, P.; Calzia, E.; Shchslavskiy, V.; Becker, W.; Rück, A. *J. Biophotonics* **2016**, 9 (8), 800–811.
- (36) Edwards, G. L.; Black, D. S.; Deacon, G. B.; Wakelin, L. P. *Can. J. Chem.* **2005**, 83 (6–7), 980–989.
- (37) Appletoq, T. G.; Pescb, J. F. J.; Wienken, M.; Menzer, S.; Lippert, B. *Inorg. Chem.* **1992**, 31 (21), 4410–4419.
- (38) Streltsov, V. A.; Epa, V. C.; James, S. A.; Caine, J. M.; Kenche, V. B.; Barnham, K. J. *Chem. Commun.* **2013**, 49, 11364–11366.
- (39) Hureau, C.; Faller, P. *Dalt. Trans.* **2014**, 43, 4233–4237.
- (40) Eryazici, I.; Moorefield, C. N.; Newkome, G. R. *Chem. Rev.* **2008**, 108 (6), 1834–1895.
- (41) Sasaki, I.; Bijani, C.; Ladeira, S.; Bourdon, V.; Faller, P.; Hureau, C. *Dalt. Trans.* **2012**, 41, 6404–6407.
- (42) Williams, J. A. G. In *Photochemistry and Photophysics of Coordination Compounds II*; Springer Berlin Heidelberg: Berlin, Heidelberg, 2007; pp 205–268.
- (43) Gauthier, M. A.; Klok, H.-A. *Chem. Commun.* **2008**, 32 (23), 2591–2611.
- (44) Rostovtsev, V. V.; Green, L. G.; Fokin, V. V.; Sharpless, K. B. *Angew. Chem. Int. Ed.* **2002**, 41 (14), 2596–2599.
- (45) Kolb, H. C.; Finn, M. G.; Sharpless, K. B. *Angew. Chem. Int. Ed.* **2001**, 40 (11), 2004–2021.
- (46) Hackenberger, C. P. R.; Schwarzer, D. *Angew. Chem. Int. Ed.* **2008**, 47 (52), 10030–10074.
- (47) Ulrich, S.; Boturyn, D.; Marra, A.; Renaudet, O.; Dumy, P. *Chem. – A Eur. J.* **2014**, 20 (1), 34–41.
- (48) Kratz, F. J. *Control. Release* **2008**, 132 (3), 171–183.
- (49) Seki, Y.; Ishiyama, T.; Sasaki, D.; Abe, J.; Sohma, Y.; Oisaki, K.; Kanai, M. *J. Am. Chem. Soc.* **2016**, 138 (34), 10798–10801.
- (50) Hershko, A.; Ciechanover, A. *Annu. Rev. Biochem.* **1998**, 67 (1), 425–479.
- (51) Pickart, C. M. *Annu. Rev. Biochem.* **2001**, 70 (1), 503–533.
- (52) Chelushkin, P. S.; Krupenya, D. V.; Tseng, Y.-J.; Kuo, T.-Y.; Chou, P.-T.; Koshevoy, I. O.; Burov, S. V.; Tunik, S. P. *Chem. Commun.* **2014**, 50 (7), 849–851.
- (53) Chelushkin, P. S.; Nukolova, N. V.; Melnikov, A. S.; Serdobintsev, P. Y.; Melnikov, P. A.; Krupenya, D. V.; Koshevoy, I. O.; Burov, S. V.; Tunik, S. P. *J. Inorg. Biochem.* **2015**, 149, 108–111.
- (54) Chelushkin, P. S.; Lysenko, E. A.; Bronich, T. K.; Eisenberg, A.; Kabanov, V. A.; Kabanov, A. V. *J. Phys. Chem. B* **2007**, 111 (29), 8419–8425.
- (55) Lakowicz, J. R. *Principles of Fluorescence Spectroscopy*, 3rd edition; Springer US: Boston, MA, 2006.
- (56) Baggaley, E.; Sazanovich, I. V.; Williams, J. A. G.; Haycock, J. W.; Botchway, S. W.; Weinstein, J. A. *RSC Adv.* **2014**, 4 (66), 35003–35008.
- (57) Rück, A.; Hauser, C.; Mosch, S.; Kalinina, S. *J. Biomed. Opt.* **2014**, 19 (9), 96005.
- (58) König, K.; Uchugonova, A.; Gorjup, E. *Microsc. Res. Tech.*

- 1  
2  
3  
4  
5  
6  
7  
8  
9  
10  
11  
12  
13  
14  
15  
16  
17  
18  
19  
20  
21  
22  
23  
24  
25  
26  
27  
28  
29  
30  
31  
32  
33  
34  
35  
36  
37  
38  
39  
40  
41  
42  
43  
44  
45  
46  
47  
48  
49  
50  
51  
52  
53  
54  
55  
56  
57  
58  
59  
60
- (59) Stringari, C.; Cinquin, A.; Cinquin, O.; Digman, M. A.; Donovan, P. J.; Gratton, E. *Proc. Natl. Acad. Sci. U. S. A.* **2011**, *108* (33), 13582–13587.
- (60) Yaseen, M. A.; Sakadžić, S.; Wu, W.; Becker, W.; Kasischke, K. A.; Boas, D. A. *Biomed. Opt. Express* **2013**, *4* (2), 307.
- (61) Blacker, T. S.; Mann, Z. F.; Gale, J. E.; Ziegler, M.; Bain, A. J.; Szabadkai, G.; Duchon, M. R. *Nat. Commun.* **2014**, *5*, 801–806.
- (62) Evans, N. D.; Gnudi, L.; Rolinski, O. J.; Birch, D. J. S.; Pickup, J. C. J. *Photochem. Photobiol. B Biol.* **2005**, *80* (2), 122–129.
- (63) Butte, P. V.; Fang, Q.; Jo, J. A.; Yong, W. H.; Pikul, B. K.; Black, K. L.; Marcu, L. J. *Biomed. Opt.* **2010**, *15* (2), 27008.
- (64) Sanchez, W. Y.; Prow, T. W.; Sanchez, W. H.; Grice, J. E.; Roberts, M. S. J. *Biomed. Opt.* **2010**, *15* (4), 46008.
- (65) Yu, J.-S.; Guo, H.-W.; Wang, C.-H.; Wei, Y.-H.; Wang, H.-W. *J. Biomed. Opt.* **2011**, *16* (3), 36008.
- (66) Gehlsen, U.; Oetke, A.; Szaszák, M.; Koop, N.; Paulsen, F.; Gebert, A.; Huettmann, G.; Steven, P. *Graefes Arch. Clin. Exp. Ophthalmol.* **2012**, *250* (9), 1293–1302.
- (67) Stringari, C.; Edwards, R. A.; Pate, K. T.; Waterman, M. L.; Donovan, P. J.; Gratton, E. *Sci. Rep.* **2012**, *2*, 309–314.
- (68) Papkovsky, D. B. *Sens. Actuators B-Chem.* **1995**, *29* (1), 213–218.
- (69) Lebedev, A. Y.; Cheprakov, A. V.; Sakadžić, S.; Boas, D. A.; Wilson, D. F.; Vinogradov, S. A. *ACS Appl. Mater. Interfaces* **2009**, *1* (6), 1292–1304.
- (70) Fercher, A.; Borisov, S. M.; Zhdanov, A. V.; Klimant, I.; Papkovsky, D. B. *ACS Nano* **2011**, *5* (7), 5499–5508.
- (71) Kurokawa, H.; Ito, H.; Inoue, M.; Tabata, K.; Sato, Y.; Yamagata, K.; Kizaka-Kondoh, S.; Kadonosono, T.; Yano, S.; Inoue, M. et al. *Sci. Rep.* **2015**, *5*, 10657.
- (72) Jin, P.; Chu, J.; Miao, Y.; Tan, J.; Zhang, S.; Zhu, W. *AIChE J.* **2013**, *59* (8), 2743–2752.
- (73) Sakadžić, S.; Roussakis, E.; Yaseen, M. A.; Mandeville, E. T.; Srinivasan, V. J.; Arai, K.; Ruvinskaya, S.; Devor, A.; Lo, E. H.; Vinogradov, S. A. et al. *Nat. Methods* **2010**, *7* (9), 755–759.
- (74) Dmitriev, R. I.; O'Donnell, N.; Papkovsky, D. B. *Bioconjug. Chem.* **2016**, *27* (2), 439–445.
- (75) Botchway, S. W.; Charnley, M.; Haycock, J. W.; Parker, A. W.; Rochester, D. L.; Weinstein, J. A.; Williams, J. A. G. *Proc. Natl. Acad. Sci. U. S. A.* **2008**, *105* (42), 16071–16076.
- (76) Saito, T.; Asakura, N.; Kamachi, T.; Okura, I. *J. Porphyr. Phthalocyanines* **2007**, *11* (3), 160–164.
- (77) Schafer, R.; Gmitro, A. F. *Biomed. Opt. Express* **2015**, *6* (2), 639.
- (78) Zhao, Q.; Zhou, X.; Cao, T.; Zhang, K. Y.; Yang, L.; Liu, S.; Liang, H.; Yang, H.; Li, F.; Huang, W. *Chem. Sci.* **2015**, *6* (3), 1825–1831.
- (79) Lazar, G. a; Desjarlais, J. R.; Handel, T. M. *Protein Sci.* **1997**, *6* (6), 1167–1178.
- (80) Godbert, N.; Pugliese, T.; Aiello, I.; Bellusci, A.; Crispini, A.; Ghedini, M. *Eur. J. Inorg. Chem.* **2007**, No. 32, 5105–5111.
- (81) Kirk, M. *SpinWorks* 3.1.3; 2010.
- (82) Brouwer, A. M. *Pure Appl. Chem.* **2011**, *83* (12), 2213–2228.
- (83) LeBel, R. G.; Goring, D. A. I. *J. Chem. Eng. Data* **1962**, *7* (1), 100–101.
- (84) Frisch, M. J.; Trucks, G. W.; Schlegel, H. B.; Scuseria, G. E.; Robb, M. A.; Cheeseman, J. R.; Scalmani, G.; Barone, V.; Mennucci, B.; Petersson, G. A. et al. *Gaussian 09, Revision D.01, Gaussian, Inc.*; 2013.
- (85) Becke, A. D. *J. Chem. Phys.* **1993**, *98* (7), 5648.
- (86) Lee, C.; Yang, W.; Parr, R. G. *Phys. Rev. B* **1988**, *37* (2), 785–789.
- (87) Stephens, P. J.; Devlin, F. J.; Chabalowski, C. F.; Frisch, M. J. *J. Phys. Chem.* **1994**, *98* (45), 11623–11627.
- (88) Andrae, D.; Haussermann, U.; Dolg, M.; Stoll, H.; Preuss, H. *Theor. Chim. Acta* **1990**, *77* (2), 123–141.
- (89) Delaglio, F.; Grzesiek, S.; Vuister, G.; Zhu, G.; Pfeifer, J.; Bax, A. J. *Biomol. NMR* **1995**, *6* (3), 277–293.
- (90) Goddard, T. D.; Kneller, D. G. *SPARKY 3, University of California, San Francisco.*

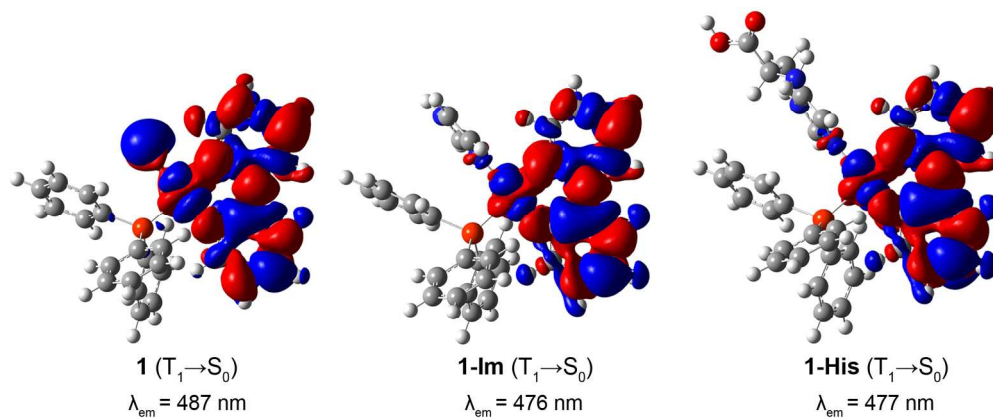




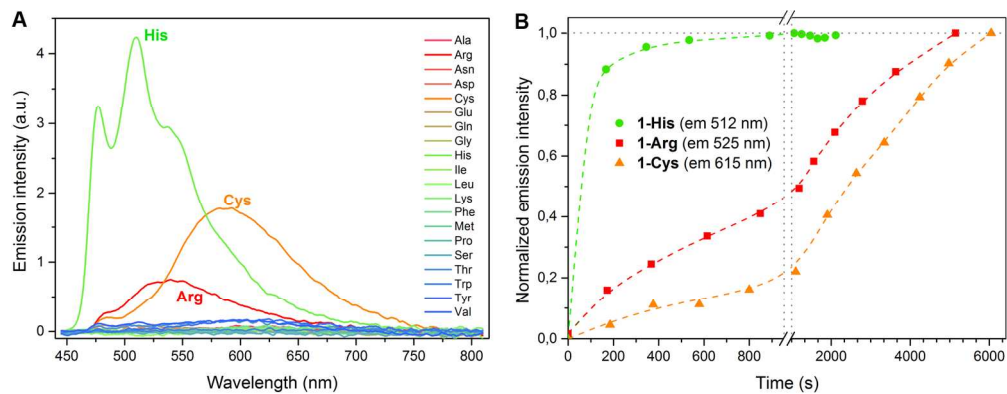
169x66mm (300 x 300 DPI)



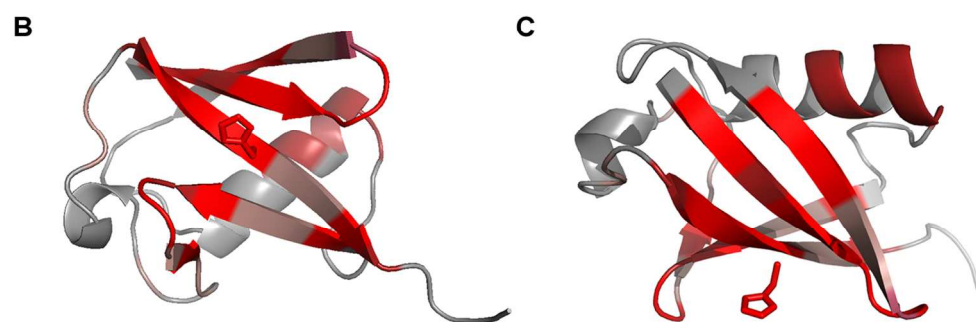
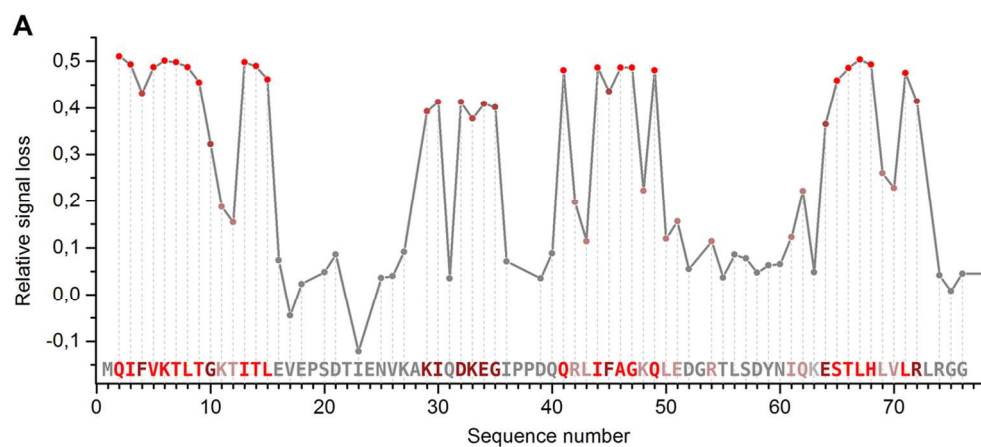
84x40mm (300 x 300 DPI)



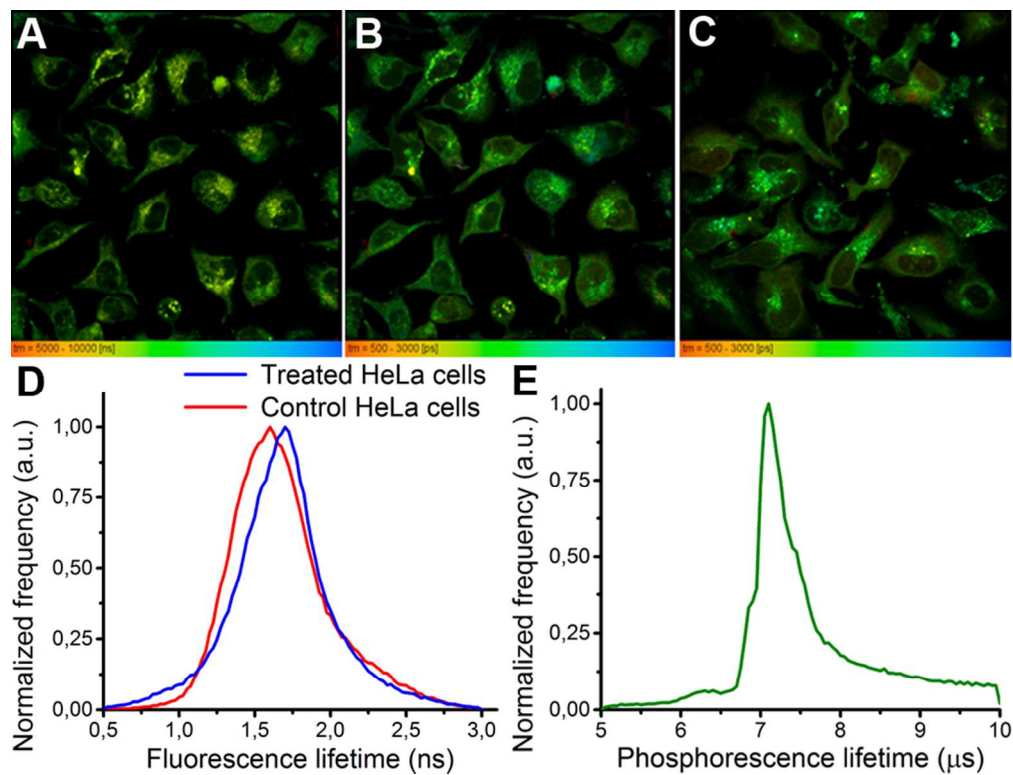
169x70mm (300 x 300 DPI)



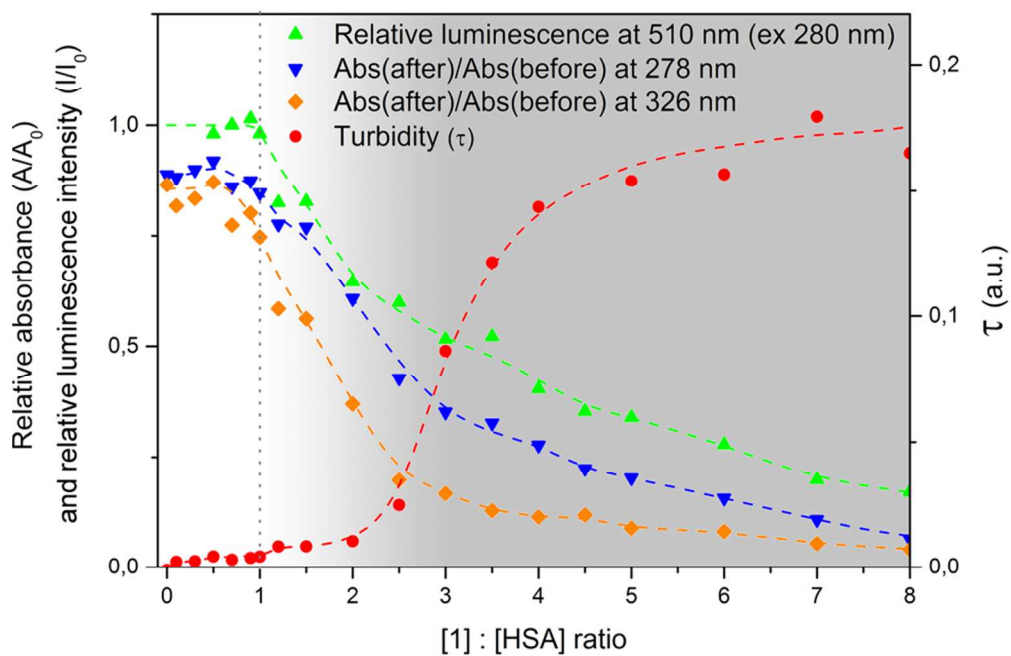
169x65mm (300 x 300 DPI)



127x100mm (300 x 300 DPI)



84x64mm (300 x 300 DPI)



84x56mm (300 x 300 DPI)